RESEARCH MEMORANDUM

MATCHING OF AUXILIARY INLETS TO SECONDARY-AIR REQUIREMENTS OF AIRCRAFT EJECTOR EXHAUST NOZZLES

By Donald P. Hearth, Gerald W. Englert, and
Kenneth L. Kowalski

Lewis Flight Propulsion Laboratory
Cleveland, Ohio

NATIONAL ADVISORY COMMITTEE
FOR AERONAUTICS
WASHINGTON
August 16, 1955

NACA RM E55D21

NATIONAL ADVISORY COMMITTEE FOR AERONAUTICS

RESEARCH MEMORANDUM

MATCHING OF AUXILIARY INLETS TO SECONDARY-AIR REQUIREMENTS OF AIRCRAFT EJECTOR EXHAUST NOZZLES

By Donald P. Hearth, Gerald W. Englert, and Kenneth L. Kowalski

SUMMARY

An analysis of the problems associated with matching secondary-air requirements of ejector exhaust nozzles and auxiliary inlets has been made for free-stream Mach numbers up to 2.0. A method for matching the components is presented.

The analysis indicated that inlets located in the free stream supply higher pressure recovery than ejectors generally require for optimum net internal thrust at Mach numbers above about 1.4. Consequently, net-thrust gains may be achieved by immersing the auxiliary inlet in a boundary layer where the inlet-momentum penalty is less.

At a free-stream Mach number of 2.0 a variable-inlet - variable-ejector configuration would develop 9.5 percent more thrust than a convergent nozzle. A fixed-inlet - fixed-ejector combination designed for a Mach number of about 1.7 would develop net thrust within 5 percent of that possible with a variable-inlet - variable-ejector system over the entire Mach number range considered (0 to 2.0).

INTRODUCTION

Increases beyond the basic jet thrust of a conventional convergent nozzle may be obtained when air taken aboard for cooling purposes is pumped through an ejector surrounding the primary nozzle (refs. 1 and 2). In a practical installation this secondary air flow may be obtained from several sources, such as the main-inlet bypass, auxiliary air inlets, or bleeds from the engine. For any such system the pressure-air-flow characteristics of the air-flow source must be matched to the pumping characteristics of the ejector.

The analysis reported herein treats the matching problems associated with the use of auxiliary air inlets which supply the secondary air for ejector-type exhaust nozzles. The importance of the inlet pressure

recovery and the inlet immersion with respect to the airframe boundary layer is evaluated. Also indicated are the net-internal-thrust gains possible with variable auxiliary inlets and ejectors as compared with fixed configurations.

ANALYSIS AND DISCUSSION

Matching Procedure

A schematic diagram of the type of system being considered is shown in figure 1. The convergent primary nozzle discharging engine gases is surrounded by an external shroud forming an ejector-type exhaust nozzle. Secondary air flow through the annulus surrounding the primary nozzle is provided by auxiliary air inlets mounted on the airframe.

At a given free-stream Mach number, internal performance of an auxiliary inlet is generally presented in terms of pressure recovery P_s/P_0 and inlet mass-flow ratio m_s/m_0 (fig. 2(a)). Ejector pumping characteristics, on the other hand, are generally not presented in terms of these same variables, but in some manner such as illustrated in figure 2(b). The variation in secondary-to-primary total-pressure ratio P_s/P_p is shown as a function of corrected weight-flow ratio $w_s\sqrt{T_s}/w_p\sqrt{T_p}$ for a given primary-nozzle pressure ratio. (Symbols are defined in appendix A.)

The equilibrium operating point of an auxiliary-inlet - ejector combination may be determined by superimposing the inlet and ejector maps. Conversion of the original maps (figs. 2(a) and (b)) to a common form is required. It appears desirable to convert inlet mass-flow ratio m_s/m_0 to corrected weight-flow ratio $w_s\sqrt{T_s}/w_p\sqrt{T_p}$ and the secondary-to-primary total-pressure ratio of the ejector P_s/P_p to pressure recovery P_s/P_0. The former conversion may be achieved by use of the following equations developed from continuity relations:

$$\frac{w_s\sqrt{T_s}}{w_p\sqrt{T_p}} = \frac{m_s}{m_0}\sqrt{\frac{T_s}{T_0}}\frac{A_c}{A_p}\frac{K_1}{P_p/P_0} \tag{1}$$

where

$$K_1 = M_0\left(1 + \frac{\gamma_0 - 1}{2}M_0^2\right)^{1/2}\left(\frac{\gamma_p + 1}{2}\right)^{\frac{\gamma_p+1}{2(\gamma_p-1)}}\sqrt{\frac{\gamma_0}{\gamma_p}} \tag{2}$$

[redacted] [redacted]

By assuming that the engine delivers a constant pressure ratio for each free-stream Mach number and that T_s/T_0 is constant, the following expression is obtained:

$$\frac{w_s\sqrt{T_s}}{w_p\sqrt{T_p}} = \frac{m_s}{m_0}\frac{A_c}{A_p}K_2 \tag{3}$$

where

$$K_2 = \frac{K_1}{\frac{P_p}{p_0}}\sqrt{\frac{T_s}{T_0}} \tag{4}$$

Conversion of the secondary-to-primary total-pressure ratio into total-pressure recovery is made by the relation

$$\frac{P_s}{P_0} = \frac{P_s}{P_p}\frac{p_0}{P_0}\frac{P_p}{p_0} \tag{5}$$

Hence, for a given free-stream Mach number the converted inlet and ejector maps would be as illustrated in figures 2(c) and (d).

An alternative technique would be to convert the ordinates and abscissas of the inlet maps to the standard notation for ejectors. Thus, the inlet-map variables would be converted to P_s/P_p and $w_s\sqrt{T_s}/w_p\sqrt{T_p}$. The same ejector map (e.g., fig. 2(b)) may then apply for all Mach numbers at which the secondary flow was choked, since the ejector pumping characteristics may be independent of P_p/p_0 for this type of operation (ref. 3).

After the component maps are converted to identical parameters ($w_s\sqrt{T_s}/w_p\sqrt{T_p}$ and P_s/P_0, e.g.), the match point can be determined as shown in figure 2(e). As indicated in equation (3), the inlet map is a function of the area ratio between the inlet and primary nozzle A_c/A_p. For case I the inlet is sized to operate critically at the match point. If the inlet were smaller (case II), it would be operated supercritically. Conversely, an oversized inlet (case III) would require subcritical operation.

For a given inlet-ejector combination, a plot such as figure 3 would be useful in determining the match points of the system over the entire flight path. The solid lines represent the pressure-recovery requirements of the ejector at free-stream Mach numbers of 0.6, 1.5, and 2.0. Since these requirements have to be satisfied, the match (equilibrium) point will fall on these lines. Critical normal-shock inlet pressure recoveries for three free-stream Mach numbers are indicated by the horizontal lines. Also shown are pressure-recovery - weight-flow schedules for critical inlet operation of three different-sized normal-shock inlets over the free-stream Mach number range studied.

[redacted]

Consider a fixed inlet sized for critical operation at a free-stream Mach number of 1.5. The operating point of the system would be at point A (fig. 3). At Mach 2.0, the inlet critical point would shift to B, since the inlet size is fixed. The system could not be operated at this point, however, for it is mismatched. The critical inlet pressure recovery is higher than required by the ejector to pass the weight flow captured by an inlet of this size. To match the ejector, the inlet would be forced to operate supercritically, point C. Conversely, if this same fixed configuration were operated at Mach 0.6, critical inlet flow would occur at point D. However, the inlet mass flow at point D is greater than that possible with the ejector for the critical inlet pressure recovery assumed. Consequently, the auxiliary inlet would be forced to operate subcritically (throat unchoked). If the subcritical pressure recovery were independent of mass-flow ratio, the match point would be at E.

In order to evaluate fully such a system as that considered in figure 3, the net propulsive force must be determined. The present study is confined to internal performance only; relative external drags have not been estimated. (External-drag differences between auxiliary inlets would probably be a very small part of the over-all thrust). In evaluating internal performance it is necessary to charge the inlet momentum of the secondary air to the system. This inlet momentum may be different from the free-stream value for unit mass flow because of the boundary layer and flow distribution on the body to which the inlet is attached. The ratio of the net ejector thrust to the net thrust of the primary nozzle is then

$$\frac{F_{n,e}}{F_{n,p}} = \frac{\frac{F_{j,e}}{F_{j,p}} - \frac{m_p V_0}{F_{j,p}}\left[1 + \frac{m_s \bar{V}}{m_p V_0} + \frac{A(p_b - p_0)}{m_p V_0}\right]}{1 - \frac{m_p V_0}{F_{j,p}}} \tag{6}$$

which becomes

$$\frac{F_{n,e}}{F_{n,p}} = \frac{\frac{F_{j,e}}{F_{j,p}} - \frac{m_p V_0}{F_{j,p}}\left[1 + \frac{\bar{V}}{V_0}\sqrt{\frac{T_p}{t_0}}\sqrt{\frac{t_0}{T_0}}\sqrt{\frac{T_0}{T_s}}\frac{w_s\sqrt{T_s}}{w_p\sqrt{T_p}} + \frac{A(p_b - p_0)}{m_p V_0}\right]}{1 - \frac{m_p V_0}{F_{j,p}}} \tag{7}$$

where $\frac{F_{j,e}}{F_{j,p}}$ comes from either experimental data or ejector theory, and

$$\frac{m_p V_0}{F_{j,p}} = \frac{\sqrt{\gamma_p \gamma_0}\,\frac{P_p}{p_0}\,M_0\sqrt{\frac{t_0}{T_p}}}{\left(\frac{\gamma_p+1}{2}\right)^{\frac{\gamma_p+1}{2(\gamma_p-1)}}\left\{\left[\left(\frac{\gamma_p+1}{2}\right)^{-\frac{\gamma_p}{\gamma_p-1}}\frac{P_p}{p_0}\right](\gamma_p+1)-1\right\}C_{F_{j,p}}} \tag{8}$$

For any free-stream Mach number, the momentum parameter $m_p V_0/F_{j,p}$ (eq. (8)) can be calculated if the flight path and engine schedule are known. Thus, the inlet momentum of the auxiliary-inlet air flow is indicated by the parameters $\sqrt{T_0/T_s}$ (assumed constant) and $\overline{V}/V_0$ where by definition

$$\overline{V} = \frac{1}{m_s}\int V_b \, dm$$

Ejector Characteristics

Before considering the over-all performance of inlet-ejector systems, a study of the characteristics of a series of typical ejectors is desirable. Such a study indicates a number of limitations on the required inlet pressure recoveries and may be useful in later analyses of the various inlet-ejector systems.

A flight plan and engine schedule have been assumed and are presented in figure 4. Acceleration to a Mach number of 0.9 would occur at sea level. The afterburner would then be turned on, the aircraft would climb to the tropopause, and would then accelerate to Mach number 2.0. The assumed nozzle-pressure-ratio schedule represents the average for several turbojet engines.

The series of 8° conical ejectors reported in references 4 and 5 was used in this study. These data were converted to required inlet pressure recovery (fig. 3) and to the net-thrust-ratio parameter defined by equation (7). The force data presented in references 4 and 5 were reduced so that they would be consistent with jet thrusts computed from mass flow and pressure data of these reference experiments. Since the ejector net-thrust ratio $F_{n,e}/F_{n,p}$ is based upon the calibrated thrust of the convergent primary nozzle, the performance of that nozzle is shown in figure 5. The step shown at Mach 0.9 is due to a change in the momentum parameter (eq. (8)) resulting from the climb phase of the assumed flight path.

The effect of weight-flow ratio and secondary-air inlet momentum on ejector net thrust is illustrated in figure 6 for a typical ejector configuration at three free-stream Mach numbers. The same ejector was used

as in the example of figure 3, and the operating points discussed therein are also indicated on figure 6. Net-thrust ratios greater than unity indicate that ejectors using auxiliary air inlets may yield net-thrust augmentations over the primary nozzle. In addition, it is interesting to note that the peak net thrust with the inlet located in the free stream ($\overline{V}/V_0 = 1.0$) occurred at a decreased weight-flow ratio as the free-stream Mach number was raised from 1.5 to 2.0. The net-thrust ratio increased and tended to peak at increasing weight-flow ratio as the secondary air was obtained from a lower-energy source (decreasing $\overline{V}/V_0$).

Presented in figure 7 are the inlet pressure recoveries required for peak net thrust of the ejectors being considered. The ejectors are designated by two groups of numbers: the first is the diameter ratio D_s/D_p, while the second group is the spacing ratio S/D_p. As Mach number was reduced, the optimum pressure recovery increased rapidly, becoming 100 percent at Mach numbers between 0.8 and 1.6, depending on the ejector and the degree of boundary-layer immersion. At Mach numbers above these values, the desired inlet pressure recovery decreases as the ejector diameter ratio is increased.

For a given ejector, the optimum pressure recovery increases as the inlet is immersed into the airframe boundary layer and decreases as the free-stream Mach number is raised. This decrease with Mach number is such that the pressure recovery that may be obtained with free-stream normal-shock inlets is greater than that required at the corresponding velocity ratio. Thus, as is apparent in figure 6, pressure recovery greater than required results in net-thrust losses. At Mach 2.0, for example, operation at the critical pressure recovery of a free-stream inlet (point F) would result in net thrust considerably below that obtainable at lower weight flows. Supercritical inlet operation would, therefore, be desirable and could be obtained with an inlet sized smaller than that required for critical inlet operation. However, it would be more desirable to reduce the critical pressure recovery by immersing the inlet in a boundary layer and, thus, obtain the added benefits of reduction in velocity ratio $\overline{V}/V_0$. The net-thrust gains resulting from boundary-layer immersion are considered when the matched inlet-ejector systems are discussed in later sections of this paper.

There are pressure-recovery limits, of course, below which the ejector does not operate and reverse flow results. As is apparent from figure 3, at a given free-stream Mach number the weight-flow ratio through the inlet-ejector combination decreases as the pressure recovery made available by the inlet decreases until zero secondary weight flow results. The minimum tolerable inlet pressure recoveries are presented in figure 8. If for a given ejector the inlet were not capable of delivering the minimum pressure recovery, gases would be emitted from the inlet, and a reverse-flow condition would be established. Operation of the ejectors so that the secondary flow was unchoked (see ref. 3) is indicated by dashed portions of the curves.

The ejector - auxiliary-inlet configuration has been treated on a net-thrust basis without regard to cooling requirements. However, minimum values of weight-flow ratio $w_s\sqrt{T_s}/w_p\sqrt{T_p}$ may be preset by necessary cooling-flow rates thereby raising the minimum allowable inlet pressure recoveries. Presented in figure 9 are the inlet pressure recoveries required for secondary weight-flow ratios of 0.03, 0.05, and 0.10.

Performance of Matched Inlet-Ejector Systems

The ejector pumping characteristics have been matched to a series of normal-shock auxiliary inlets. The performance of these inlets (fig. 10) has been computed by the stream-filament method of appendix B. The flow ahead of the inlet was represented by a single filament of the boundary layer having a uniform velocity profile. Included in appendix B are the calculating techniques required for finite-sized inlets having nonuniform entering profiles such as would exist with actual boundary-layer inlets.

The results of matching the series of ejectors reported in references 4 and 5 to variable inlets are shown in figures 11 and 12. For these curves, the inlet size and depth of immersion in the boundary layer were varied for each condition to yield the maximum net thrust. Peak net thrust obtainable with a variable-inlet - variable-ejector system is the envelope of the individual fixed-ejector net-thrust curves.

For a variable-inlet - variable-diameter-ratio-ejector combination (constant spacing ratio of 0.80, fig. 11), net-thrust augmentation as high as 9.5 percent could result at a free-stream Mach number of 2.0, and weight-flow ratios of at least 0.025 would be obtained as Mach number was raised from 0 to 2.0. If, instead of a completely variable system, a fixed-ejector - variable-inlet configuration were used, the 1.20-0.80 ejector would be the best compromise. This observation, as well as the relative superiority of ejectors with small (1.10) and large (1.40) diameter ratios at the various Mach numbers, is similar to that noted from unmatched-ejector analysis (ref. 2). The effect of spacing ratios on net thrust and secondary weight flow is indicated in figure 12. A reduction in spacing ratio from 0.80 to 0.40 may be desirable at Mach numbers between 1.2 and 1.9. It was found in obtaining figures 11 and 12 that for Mach numbers in excess of about 1.2 the inlet should be placed deeper in the boundary layer as Mach number increased. At Mach numbers of 1.2 and below, the net thrusts appeared to be unaffected by the position of the inlet in the boundary layer.

The performance of fixed inlets matched to variable ejectors is shown in figure 13. Included for comparison is the performance with a completely variable system (fig. 11). The ejector spacing ratio was maintained at 0.80 and the diameter ratio was varied to obtain maximum

thrust with each inlet design. Only results for inlets having design points at free-stream Mach numbers of 1.5, 1.7, and 2.0 are plotted. The thrust and weight-flow results for design Mach numbers of 0.6, 0.9, and 1.2 fall within the curves presented. An inlet designed for a Mach number of 1.7 represents a good compromise over the assumed flight plan.

If the inlet and ejector were both of fixed geometry, the performance shown in figure 14 would result. A fixed inlet designed for a Mach number of 1.7 and matched to the 1.20-0.80 ejector of figure 14(b) appears as the best fixed configuration over the entire Mach number range. Such a fixed configuration would provide net internal thrusts within 5 percent of the peak performance of a variable-inlet and variable-ejector combination. Secondary-to-primary weight-flow ratios of at least 0.04 are obtainable from take-off to a free-stream Mach number of 2.0 with this fixed configuration.

If the auxiliary inlet were located in the free stream, the performance shown in figure 15 would be obtained. Because of the high inlet momentum associated with the free-stream inlet and the ability of the ejector to better utilize the lower pressure recovery of boundary-layer inlets, the best variable-ejector - free-stream-inlet combination would have up to 4 percent less net thrust (at $M_0 = 2.0$) than the best variable-ejector - boundary-layer-inlet combination.

It was assumed for the inlet calculations that there was a 5-percent total-pressure loss in the subsonic portion of the inlet; however, higher losses due to duct bends, dumping losses, and so forth, may occur. The effect of subsonic duct pressure recovery on the performance of the optimum fixed configuration (ejector, 1.20-0.80; inlet designed for free-stream Mach number, 1.7) is shown in figure 16. If the inlet were operating supercritically, the additional losses would have no effect on either net thrust or weight-flow ratio (as at Mach 2.0 for up to 10-percent loss). With a loss greater than 10 percent at Mach 2.0, the net thrust increased, since the optimum weight flow was approached. At Mach numbers of 1.5 and below, the net-thrust losses were slight, dropping 2.5 percent at a Mach number of 0.9 as the internal pressure losses increased from 5 to 20 percent. The corresponding weight-flow reduction was from 0.056 to 0.022.

SUMMARY OF RESULTS

An analytical method is presented for matching secondary-air requirements of ejector exhaust nozzles to normal-shock auxiliary air inlets. This method was used to study a series of 8° conical ejectors for which experimental data were available in combination with a group of auxiliary inlets. Within the range of variables considered, the following results were noted:

1. An auxiliary inlet-ejector configuration can develop up to 9.5 percent more net thrust than a convergent nozzle at a free-stream Mach number of 2.0.

2. A fixed inlet-ejector combination can develop within 5 percent of the net thrust obtainable with variable-inlet - variable-ejector systems from take-off to a free-stream Mach number of 2.0.

3. Free-stream inlets generally supply a higher pressure recovery than that required for optimum net-thrust performance of ejectors above free-stream Mach numbers of about 1.4. Net-thrust gains of about 4 percent may be obtained by immersing the auxiliary inlet into the airframe boundary layer.

4. Properly matched inlet-ejector systems would deliver secondary weight-flow ratios of at least 0.025 at free-stream Mach numbers from 0 to 2.0.

Lewis Flight Propulsion Laboratory
National Advisory Committee for Aeronautics
Cleveland, Ohio, April 25, 1955

[redacted]

APPENDIX A

SYMBOLS

The following symbols are used in this report:

A	area, sq ft
A_c	inlet cowl area, sq ft
A_c'	cross-sectional area of undisturbed flow which eventually enters auxiliary inlet, sq ft
$\frac{A_c}{A_p}$	ratio of inlet cowl area to primary-nozzle throat area
$C_{F_{j,p}}$	ratio of measured primary to computed sonic nozzle jet thrust, $\frac{F_{j,p}}{p_p A_p(\gamma + 1) - p_0 A_p}$
D	diameter, ft
$\frac{D_s}{D_p}$	ejector diameter ratio
$F_{j,e}$	ejector jet thrust, lb
$F_{j,p}$	primary jet thrust, lb
$F_{n,e}$	ejector net thrust, $F_{j,e} - [m_s\bar{V} + m_p V_0 + A(p_b - p_0)]$, lb
$F_{n,p}$	primary net thrust, $F_{j,p} - m_p V_0$, lb
$F_{n,p,i}$	ideal primary net thrust, $m_p(V_i - V_0)$, lb
h	height of finite inlet, ft
K_1	defined in eq. (2)
K_2	defined in eq. (4)
M	Mach number
m	mass flow, ρAV, slugs/sec

3666

$\frac{m_s}{m_o}$	auxiliary-inlet mass-flow ratio
P	total pressure, lb/sq ft
$\frac{P_B}{P_A}$	total-pressure ratio across a normal shock
$\frac{P_p}{P_o}$	primary-nozzle pressure ratio
$\frac{P_s}{P_o}$	total-pressure recovery of auxiliary inlet
p	static pressure, lb/sq ft
$\frac{S}{D_p}$	ejector spacing ratio
T	total temperature, ^oR
t	static temperature, ^oR
V	velocity, ft/sec
$\overline{V}$	mean effective velocity of fluid in boundary layer captured by auxiliary inlet, ft/sec
$\frac{w_s\sqrt{T_s}}{w_p\sqrt{T_p}}$	ejector corrected weight-flow ratio
y	distance from surface to point in boundary layer, ft
γ	ratio of specific heats
δ	boundary-layer thickness, ft
ρ	static density, slugs/cu ft

Subscripts:

b	conditions in boundary layer
i	ideal

[redacted]

p	primary
s	secondary
0	free stream
1	lower lip of two-dimensional inlet
2	upper lip of two-dimensional inlet

3666

APPENDIX B

CALCULATION OF INLET PERFORMANCE

Stream-Filament Calculation

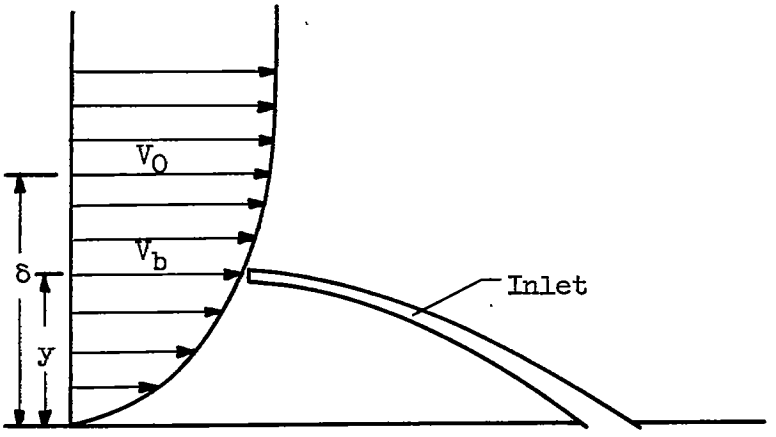

Sketch (a)

The inlet performance presented in figure 10 has been computed under the following assumptions:

(1) The flow conditions ahead of the inlet (sketch (a)) may be represented by a single stream filament of the boundary layer.

(2) Boundary-layer profile is defined by

$$\frac{V_b}{V_0} = \left(\frac{y}{\delta}\right)^{1/7}$$

(3) Static pressure in the boundary layer is equal to free-stream static pressure.

(4) Subsonic-diffuser pressure recovery is equal to a constant value, 0.95.

(5) Ratio of specific heats $\gamma = 1.40$.

(6) Total temperature is constant.

Using the perfect-gas law in conjunction with assumptions (2), (3), (5), and (6) gives

$$\frac{\rho_0}{\rho_b} = \frac{t_b}{t_0} = \frac{T_0}{t_0} - \frac{\gamma - 1}{2}\left(\frac{V_b}{V_0}\right)^2 M_0^2$$

$$= 1 + \frac{\gamma - 1}{2} M_0^2 \left[1 - \left(\frac{y}{\delta}\right)^{2/7}\right] \tag{B1}$$

The inlet critical mass-flow ratio is

$$\frac{m_s}{m_0} = \frac{\rho_b V_b \left(\frac{A_c'}{A_c}\right)_b}{\rho_0 V_0 \left(\frac{A_c'}{A_c}\right)_0} \tag{B2}$$

where

$$\frac{A_c'}{A_c} = \frac{1}{M}\left(\frac{1 + \frac{\gamma - 1}{2} M^2}{\frac{\gamma + 1}{2}}\right)^{\frac{\gamma+1}{2(\gamma-1)}} \qquad \text{if } M < 1.0$$

$$= 1.0 \qquad \text{if } M \geq 1.0$$

Substituting equation (B1) into (B2) yields

$$\frac{m_s}{m_0} = \frac{(A_c'/A_c)_b}{(A_c'/A_c)_0} \frac{\left(\frac{y}{\delta}\right)^{1/7}}{1 + \frac{\gamma - 1}{2} M_0^2 \left[1 - \left(\frac{y}{\delta}\right)^{2/7}\right]} \tag{B3}$$

The inlet total-pressure recovery can be found from

$$\frac{P_s}{P_0} = 0.95\left(\frac{P_b}{P_0}\right)\left(\frac{P_B}{P_A}\right)_{\text{at } M_b} \tag{B4}$$

which may be written as

$$\frac{P_s}{P_0} = 0.95 \frac{\left(1 + \frac{\gamma - 1}{2} M_b^2\right)^{\frac{\gamma}{\gamma-1}}}{\left(1 + \frac{\gamma - 1}{2} M_0^2\right)^{\frac{\gamma}{\gamma-1}}} \left(\frac{P_B}{P_A}\right)_{\text{at } M_b} \tag{B5}$$

[redacted]

Calculation for Inlets Having Nonuniform Entering Profiles

The inlets used in the body of the report were all computed by the preceding analysis, in which the flow conditions ahead of the inlet were considered to be represented by a single stream filament of the boundary layer. These infinitesimal inlets are less representative of actual finite inlets when the ratio h/δ is no longer close to zero or when y/δ is less than or equal to 1. In order to see how the results of this analysis pertain to boundary-layer-immersed inlets of a larger size, the following calculations were made: Inlet performance was computed for a series of two-dimensional inlets having nonuniform entering profiles.

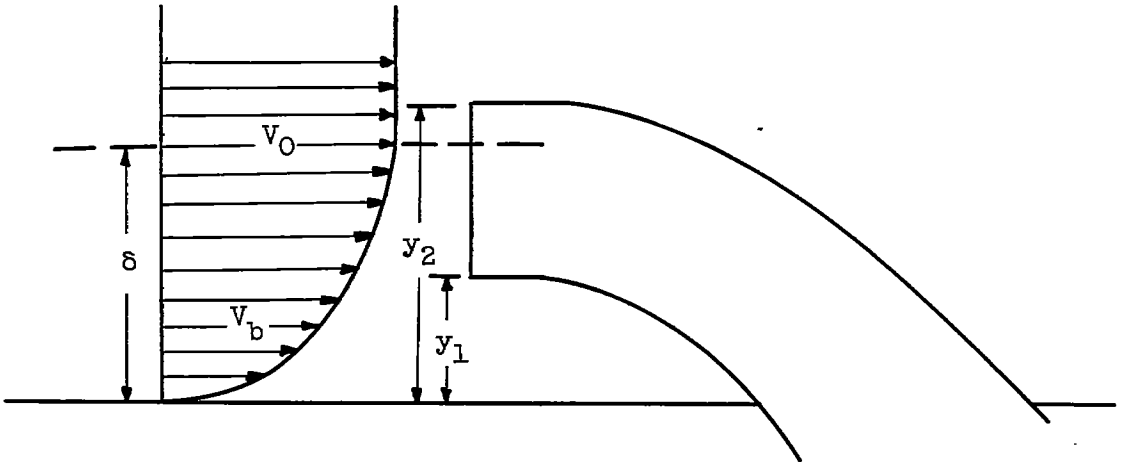

Sketch (b)

It was assumed that

(1) The inlet captures a stream tube of cross-sectional area equal to that of the inlet (sketch (b)).

(2) Boundary-layer profile is defined by

$$\frac{V_b}{V_0} = \left(\frac{y}{\delta}\right)^{1/7}$$

(3) Static pressure in the boundary layer is equal to the free-stream static pressure.

(4) Mixing occurs in a constant-area section until a flow of uniform profile is attained.

[redacted]

(5) Ratio of specific heats $\gamma = 1.40$.

(6) Total temperature is constant.

Consider a two-dimensional inlet (total cowl area per unit width $= y_2 - y_1$) a portion of which is immersed in the boundary layer (immersed area per unit width $= \delta - y_1$). Then, $y_2 > \delta$.

If assumption (1) is used, the inlet mass-flow ratio can be expressed as

$$\frac{m_s}{m_0} = \frac{\int_{y_1}^{\delta} \rho_b V_b \, dy + \rho_0 V_0 (y_2 - \delta)}{\rho_0 V_0 (y_2 - y_1)} \tag{B6}$$

With assumptions (1) and (2), equation (B6) becomes

$$\frac{m_s}{m_0} = \frac{1}{y_2 - y_1} \int_{y_1}^{\delta} \frac{\left(\frac{y}{\delta}\right)^{1/7}}{1 + \frac{\gamma - 1}{2} M_0^2 \left[1 - \left(\frac{y}{\delta}\right)^{2/7}\right]} \, dy + \frac{y_2 - \delta}{y_2 - y_1} \tag{B7}$$

By equating the capture mass flow in the boundary layer to the mass flow at the uniform-profile station, the following may be obtained:

$$\frac{P_s}{P_0} \frac{M_s}{M_0} \left[\frac{1 + \frac{\gamma - 1}{2} M_0^2}{1 + \frac{\gamma - 1}{2} M_s^2}\right]^{\frac{\gamma+1}{2(\gamma-1)}} = \frac{1}{y_2 - y_1} \left\{ \int_{y_1}^{\delta} \frac{\left(\frac{y}{\delta}\right)^{1/7}}{1 + \frac{\gamma - 1}{2} M_0^2 \left[1 - \left(\frac{y}{\delta}\right)^{2/7}\right]} \, dy + \frac{y_2 - \delta}{y_2 - y_1} \right\} \tag{B8}$$

Equating momentum at the uniform-profile and boundary-layer stations yields

$$p_s (1 + \gamma M_s^2)(y_2 - y_1) = p_0 \left[\int_{y_1}^{\delta} (1 + \gamma M_b^2) dy + (1 + \gamma M_0^2)(y_2 - \delta) \right]$$

and, since $\frac{p}{P} = \frac{1}{\left(1 + \frac{\gamma - 1}{2} M^2\right)^{\frac{\gamma}{\gamma-1}}}$,

$$\frac{P_s}{P_0}(1 + \gamma M_s^2)\left(\frac{1 + \frac{\gamma - 1}{2} M_0^2}{1 + \frac{\gamma - 1}{2} M_s^2}\right)^{\frac{\gamma}{\gamma-1}} = \frac{1}{y_2 - y_1}\left[\int_{y_1}^{\delta} (1 + \gamma M_b^2)dy + (1 + \gamma M_0^2)(y_2 - \delta)\right] \quad \text{(B9)}$$

Under assumptions (2) and (6),

$$M_b^2 = \frac{M_0^2\left(\frac{y}{\delta}\right)^{2/7}}{1 + \frac{\gamma - 1}{2} M_0^2\left[1 - \left(\frac{y}{\delta}\right)^{2/7}\right]}$$

Equation (B9) may then be written as

$$\frac{P_s}{P_0}(1+\gamma M_s^2)\left[\frac{1 + \frac{\gamma - 1}{2} M_0^2}{1 + \frac{\gamma - 1}{2} M_s^2}\right]^{\frac{\gamma}{\gamma-1}} = \frac{1}{y_2 - y_1}\left(\int_{y_1}^{\delta}\left\{1 + \frac{\gamma M_0^2\left(\frac{y}{\delta}\right)^{2/7}}{1+\frac{\gamma - 1}{2} M_0^2\left[1-\left(\frac{y}{\delta}\right)^{2/7}\right]}\right\}dy + (1 + \gamma M_0^2)(y_2 - \delta)\right) \quad \text{(B10)}$$

Simultaneous solution of equations (B8) and (B10) yields two solutions for conditions after mixing. The supersonic solution, $M_s > 1$, corresponds to changing a nonuniform supersonic flow to a one-dimensional flow with no shock encountered. The subsonic solution, $M_s < 1$, corresponds to conditions behind the normal shock from which the inlet pressure recovery may be obtained if the appropriate subsonic duct loss is applied. If the inlet is completely immersed in the boundary layer so that $y_2 < \delta$, equations (B7), (B8), and (B10) become, respectively,

$$\frac{m_s}{m_0} = \frac{1}{y_2 - y_1}\int_{y_1}^{y_2} \frac{\left(\frac{y}{\delta}\right)^{1/7}}{1 + \frac{\gamma - 1}{2} M_0^2\left[1 - \left(\frac{y}{\delta}\right)^{2/7}\right]} dy \quad \text{(B11)}$$

$$\frac{P_s}{P_0}\frac{M_s}{M_0}\left(\frac{1+\frac{\gamma-1}{2}M_0^2}{1+\frac{\gamma-1}{2}M_s^2}\right)^{\frac{\gamma+1}{2(\gamma-1)}} = \frac{1}{y_2-y_1}\int_{y_1}^{y_2}\frac{\left(\frac{y}{\delta}\right)^{1/7}}{1+\frac{\gamma-1}{2}M_0^2\left[1-\left(\frac{y}{\delta}\right)^{2/7}\right]}\,dy \tag{B12}$$

and

$$\frac{P_s}{P_0}\left(1+\gamma M_s^2\right)\left(\frac{1+\frac{\gamma-1}{2}M_0^2}{1+\frac{\gamma-1}{2}M_s^2}\right)^{\frac{\gamma}{\gamma-1}} = \frac{1}{y_2-y_1}\int_{y_1}^{y_2}1+\frac{\gamma M_0^2\left(\frac{y}{\delta}\right)^{2/7}}{1+\frac{\gamma-1}{2}M_0^2\left[1-\left(\frac{y}{\delta}\right)^{2/7}\right]}\,dy \tag{B13}$$

3666

Correlation of Filament and Cowl-Lip Positions

Mass-flow and pressure-recovery characteristics for attached ($y_1 = 0$) and unattached ($y_1 > 0$) inlets having nonuniform entering profiles were computed by use of equations (B7), (B8), (B10), (B11), (B12), and (B13). The positions of the stream filament for the same pressure recovery and mass-flow ratio as these inlets were determined by comparison of these results with results of equations (B3) and (B4) and are shown in figures 17 and 18.

These curves give some indication of the accuracy involved in adapting the results of the matching analysis, which was based on an infinitesimal inlet, to a given finite inlet. Where the dashed and solid lines coincide in figures 17 and 18, both mass-flow and pressure-recovery criteria can be satisfied by the adjustment of effective y/δ. The results of the matching analysis would be the same in this case if the inlet considered were either infinitesimal or of the sizes indicated on the curves. However, the inlet would be operating at a different boundary-layer position. In general, the distance between the dashed and solid lines was small, and conversion to finite-sized inlet appears reasonable within the range of variables presented in figures 17 and 18.

REFERENCES

1. Samuels, John C., and Yanowitz, Herbert: Analysis of Several Methods of Pumping Cooling Air for Turbojet-Engine Afterburners. NACA RM E52K26, 1953.

2. Fleming, William A.: Internal Performance of Several Types of Jet-Exit Configurations for Supersonic Turbojet Aircraft. NACA RM E52K04, 1953.

3. Kochendorfer, Fred D., and Rousso, Morris D.: Performance Characteristics of Aircraft Cooling Ejectors Having Short Cylindrical Shrouds. NACA RM E51E01, 1951.

4. Greathouse, W. K., and Hollister, D. P.: Preliminary Air-Flow and Thrust Calibrations of Several Conical Cooling-Air Ejectors with a Primary to Secondary Temperature Ratio of 1.0. I - Diameter Ratios of 1.21 and 1.10. NACA RM E52E21, 1952.

5. Greathouse, W. K., and Hollister, D. P.: Preliminary Air-Flow and Thrust Calibrations of Several Conical Cooling-Air Ejectors with a Primary to Secondary Temperature Ratio of 1.0. II - Diameter Ratios of 1.06 and 1.40. NACA RM E52F26, 1952.

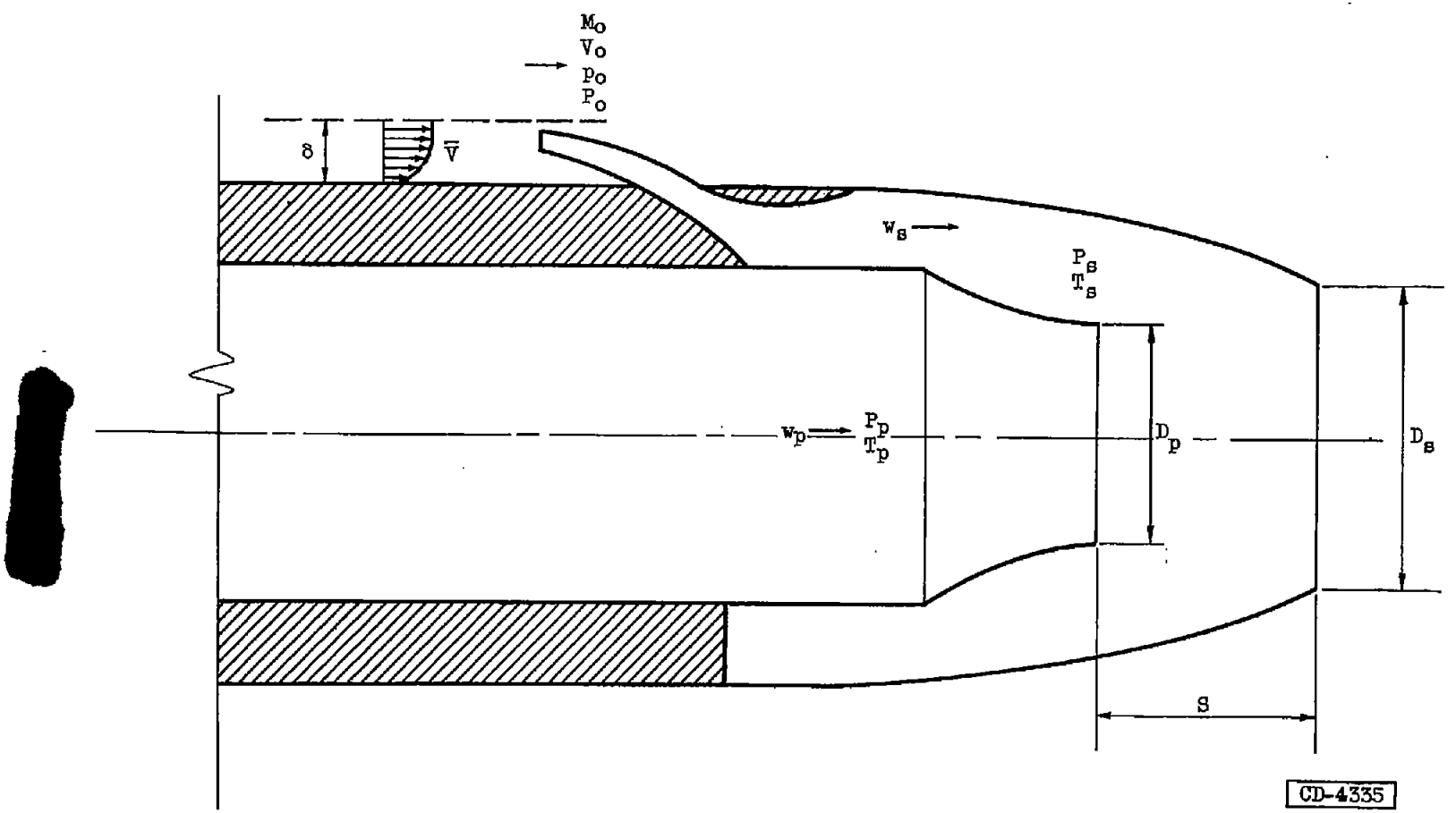

Figure 1. - Example of installation having auxiliary-inlet - ejector exhaust nozzle.

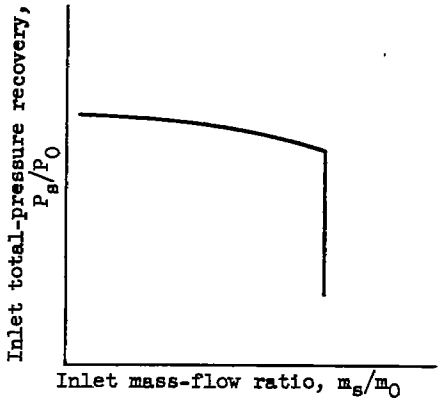

(a) Usual inlet map.

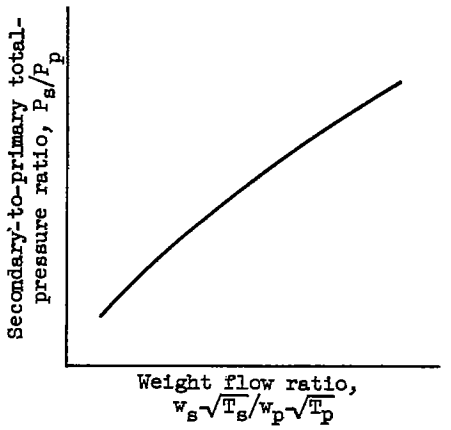

(b) Usual ejector map. Constant primary-nozzle pressure ratio.

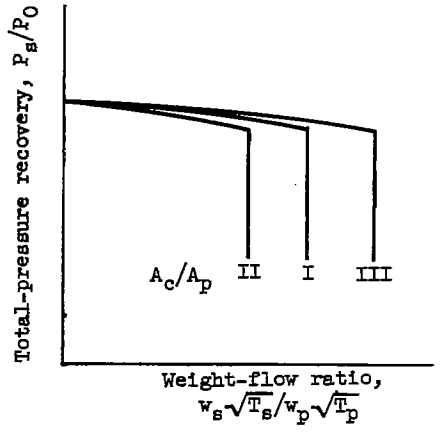

(c) Converted inlet map.

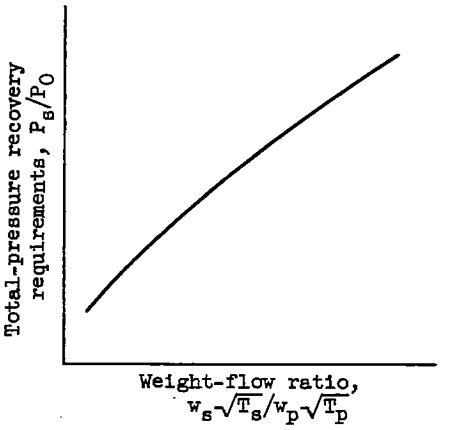

(d) Converted ejector map. Constant primary-nozzle pressure ratio.

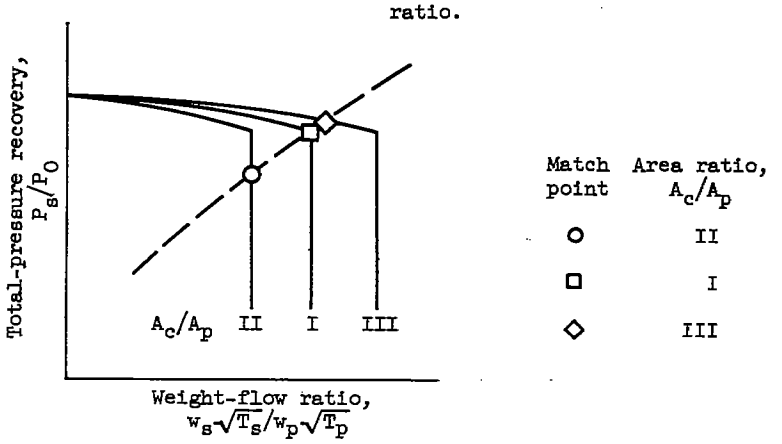

(e) Determination of match point.

Figure 2. - Example of conversion of usual performance maps for matching at a constant flight Mach number.

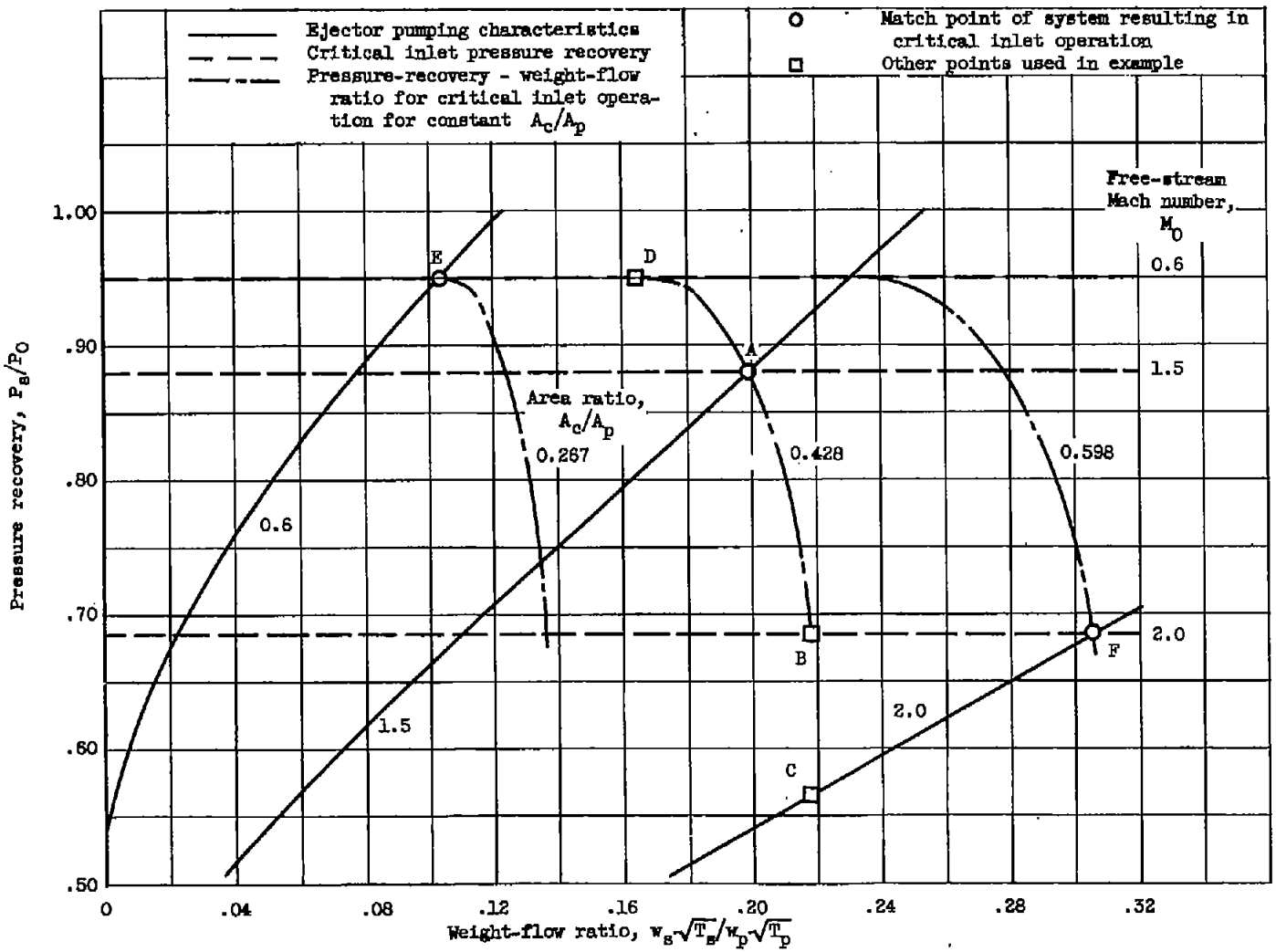

Figure 3. - Example of generalized map for match-point determination. Ejector diameter ratio, 1.20; ejector spacing ratio, 0.80; free-stream normal-shock inlet with 5-percent subsonic diffuser loss.

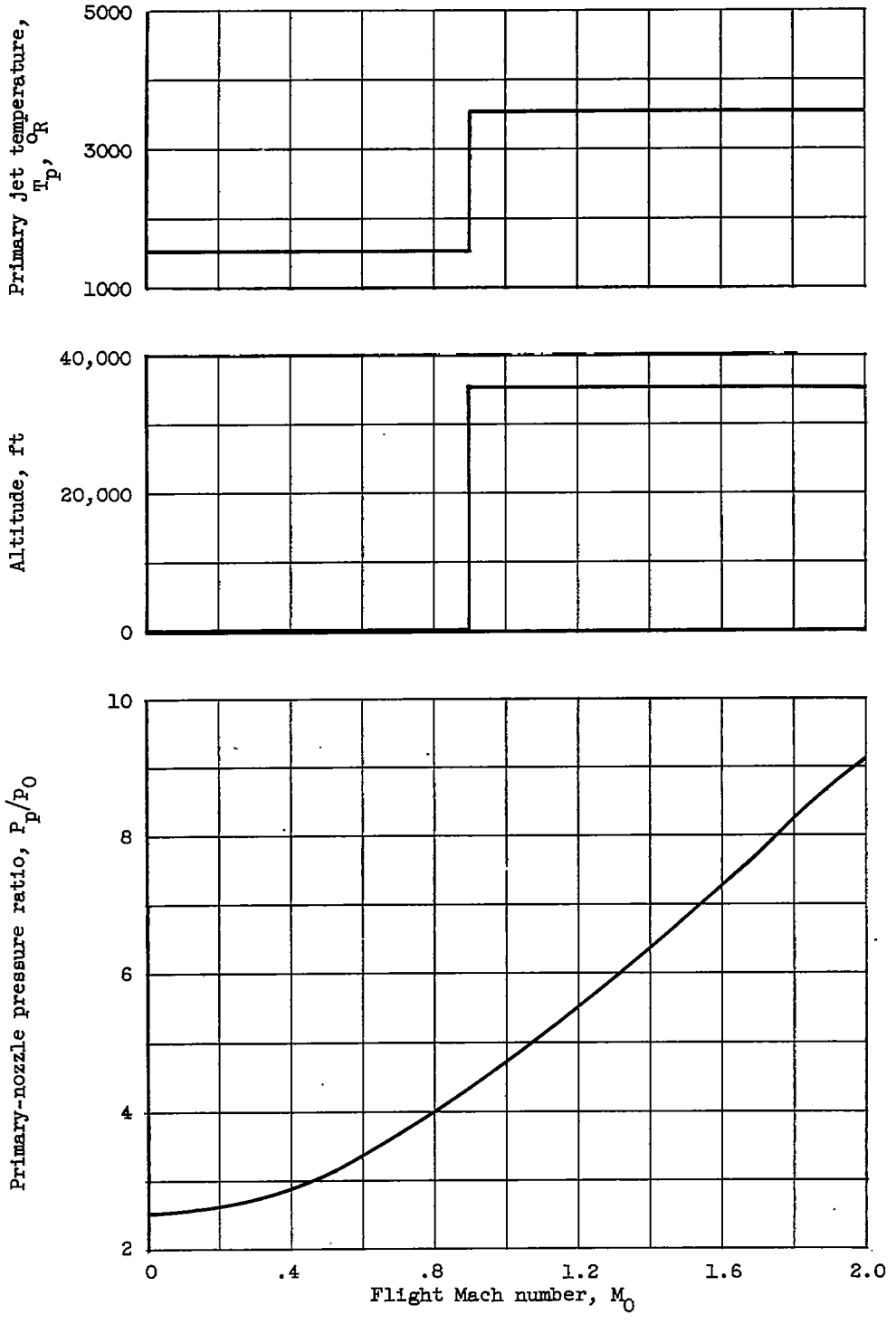

Figure 4. - Assumed engine schedule and flight plan.

[redacted]

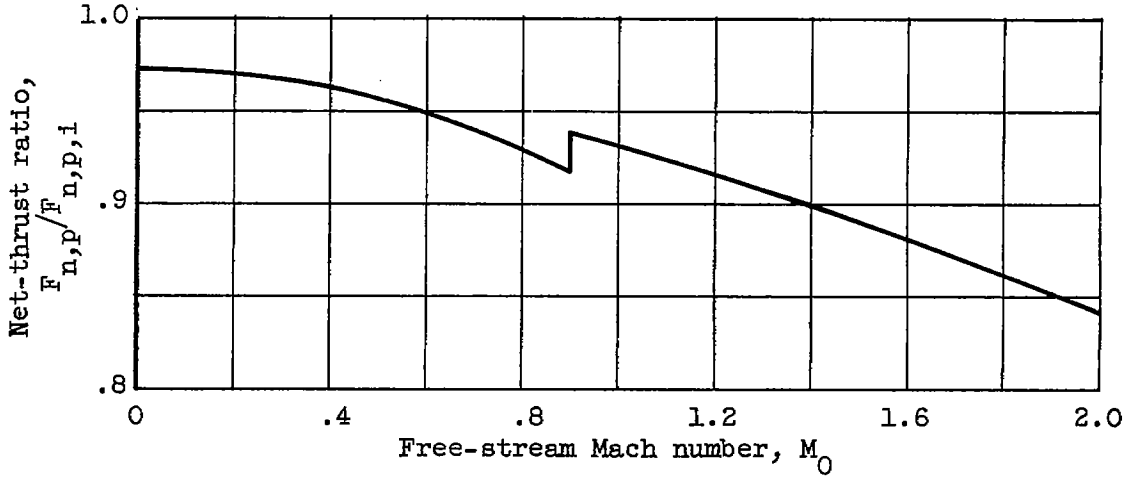

Figure 5. - Performance of primary nozzle used within ejectors studied. Net-thrust ratio based on complete isentropic expansion.

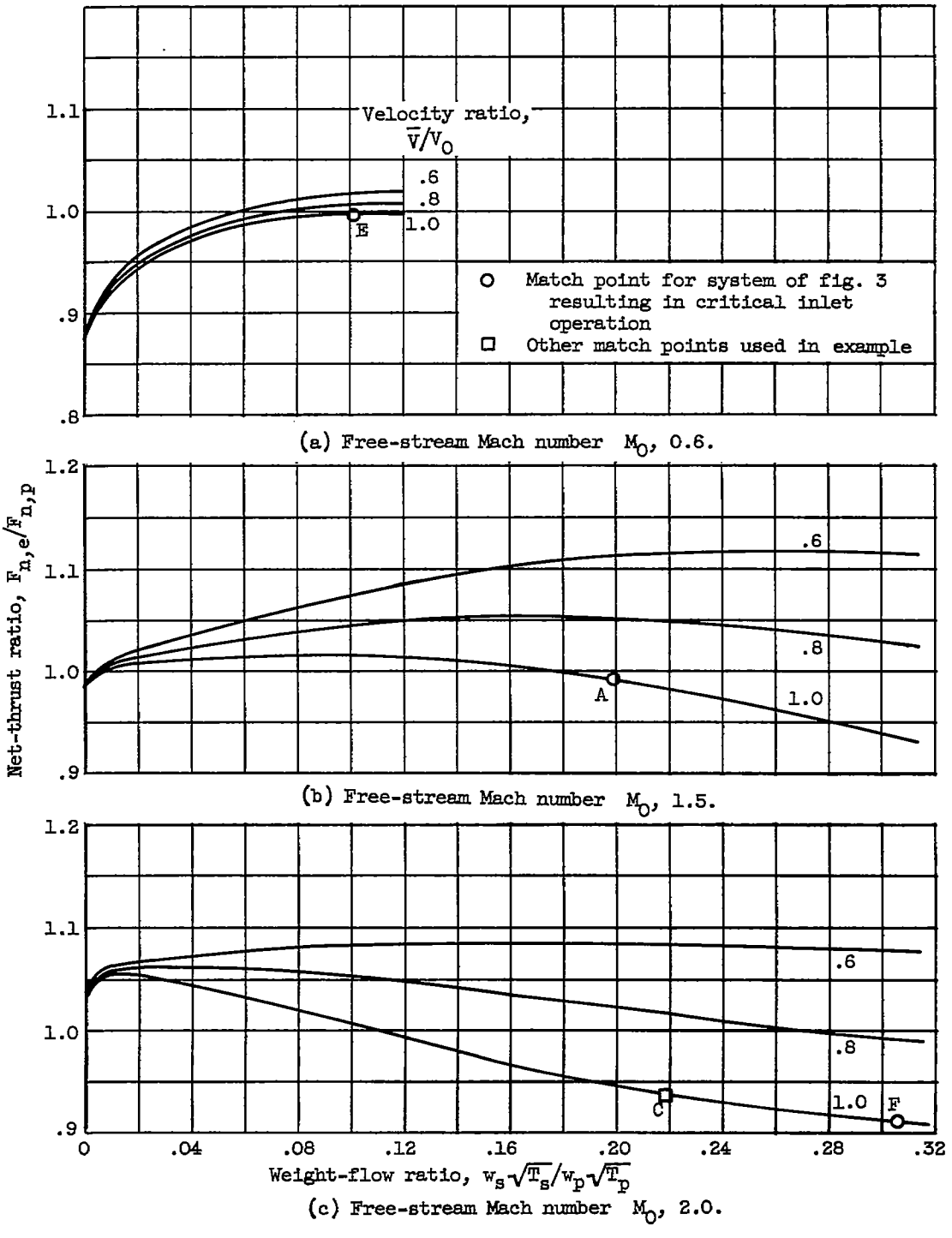

Figure 6. - Effect of inlet momentum and secondary-weight-flow ratio on ejector net thrust. Diameter ratio, 1.2; spacing ratio, 0.80; points A, C, E, and F from figure 3.

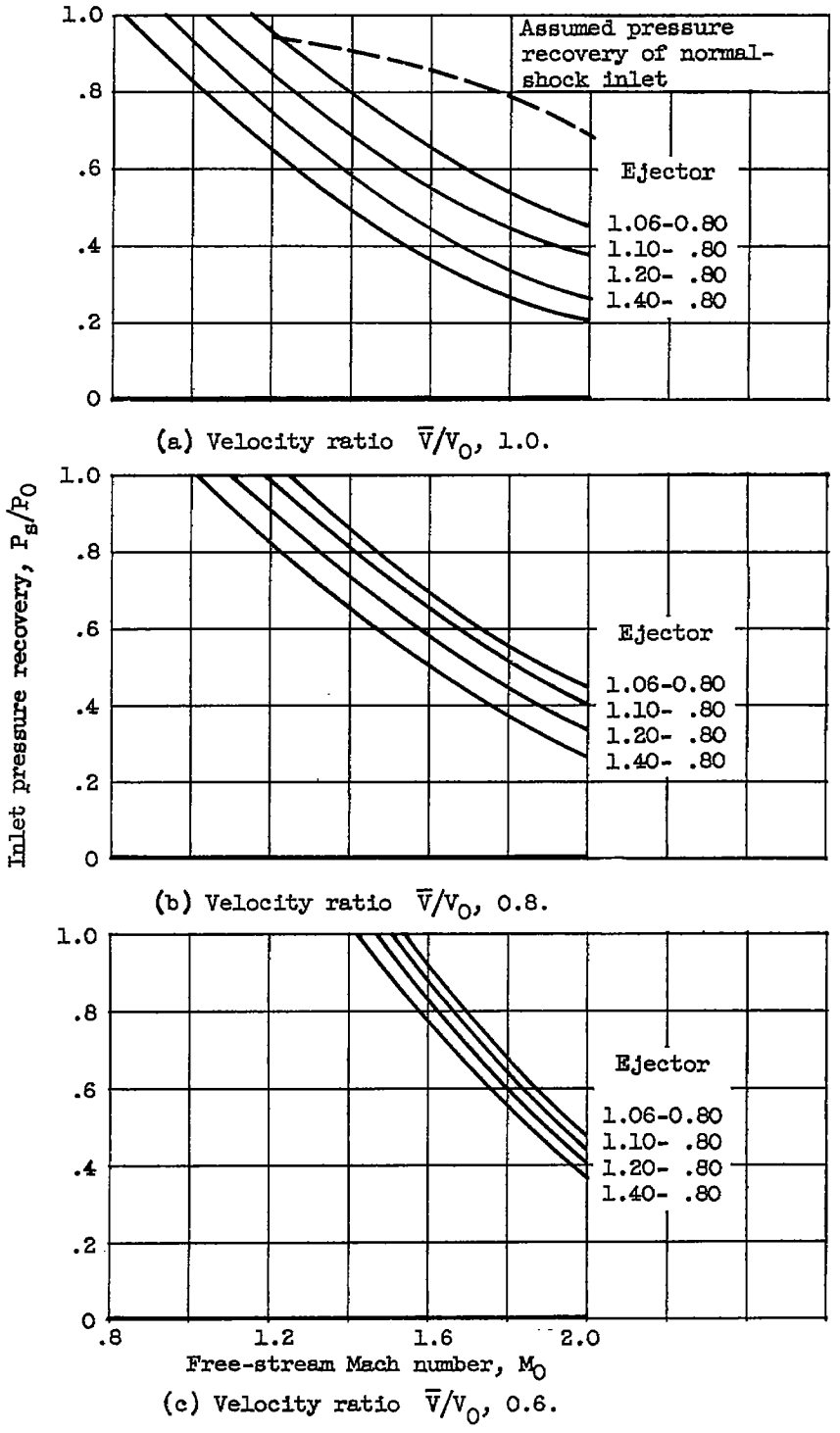

(a) Velocity ratio $\overline{V}/V_0$, 1.0.

(b) Velocity ratio $\overline{V}/V_0$, 0.8.

(c) Velocity ratio $\overline{V}/V_0$, 0.6.

Figure 7. - Inlet pressure recovery required for peak net thrust at various velocity ratios.

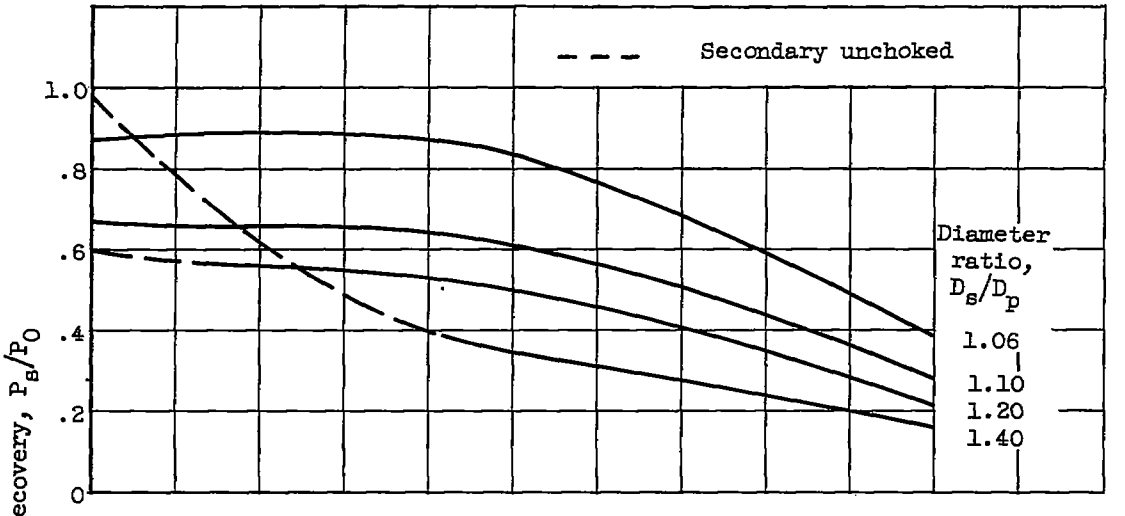

(a) Effect of diameter ratio. Spacing ratio, 0.80.

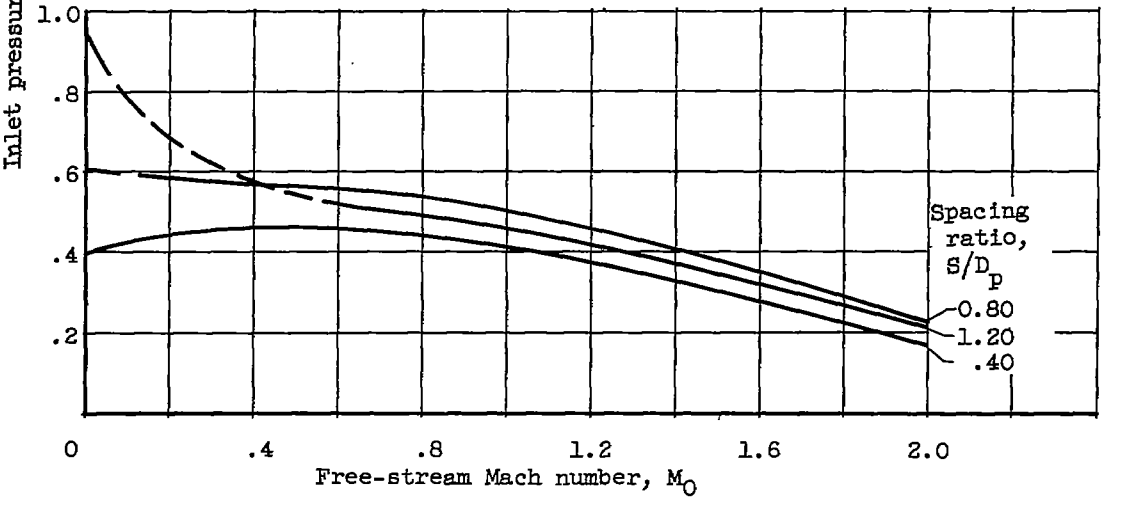

(b) Effect of spacing ratio. Diameter ratio, 1.20.

Figure 8. - Minimum inlet pressure recovery without reverse flow.

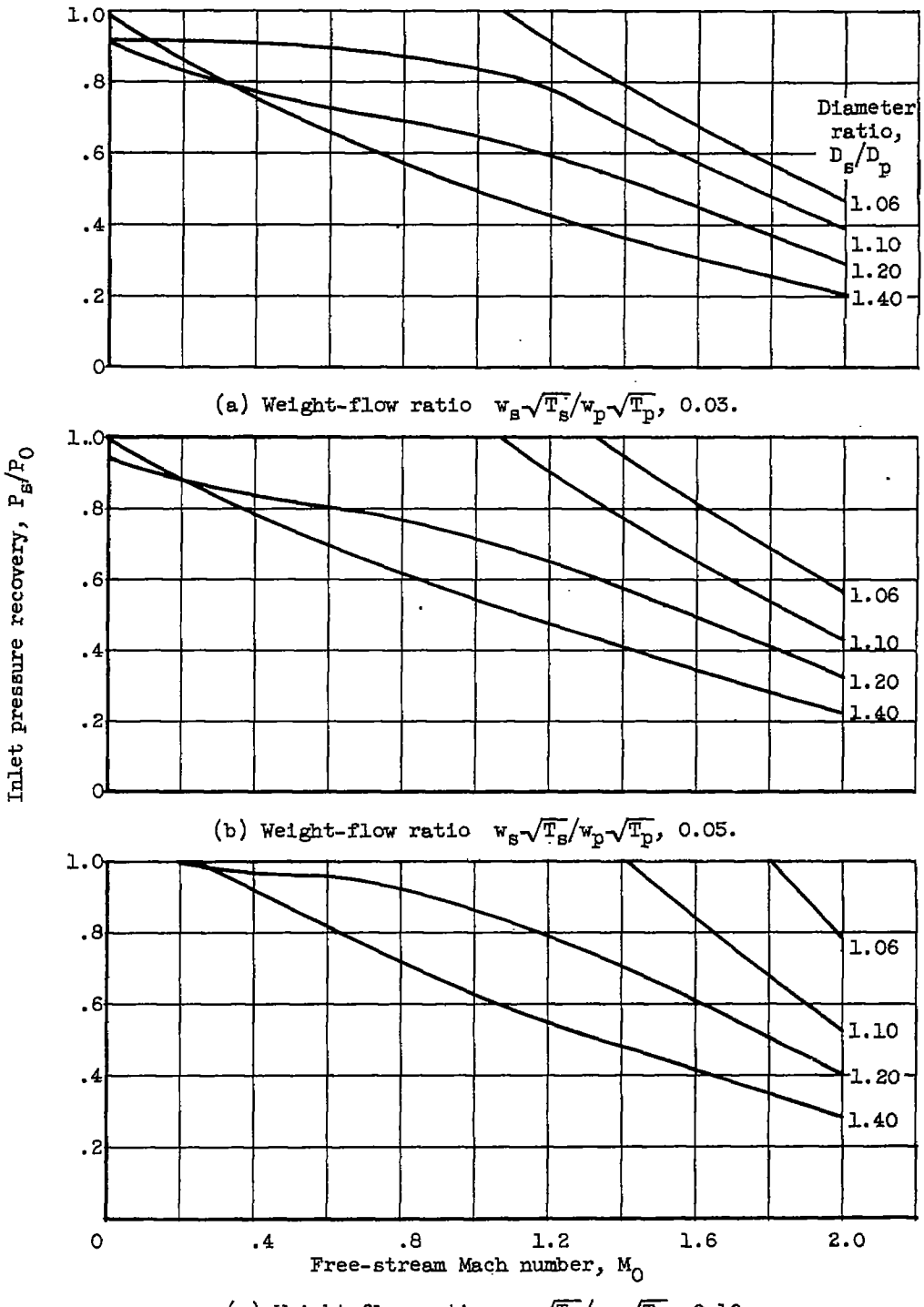

(a) Weight-flow ratio $w_s\sqrt{T_s}/w_p\sqrt{T_p}$, 0.03.

(b) Weight-flow ratio $w_s\sqrt{T_s}/w_p\sqrt{T_p}$, 0.05.

(c) Weight-flow ratio, $w_s\sqrt{T_s}/w_p\sqrt{T_p}$, 0.10.

Figure 9. - Inlet pressure recovery required for various weight-flow ratios. Spacing ratio, 0.80.

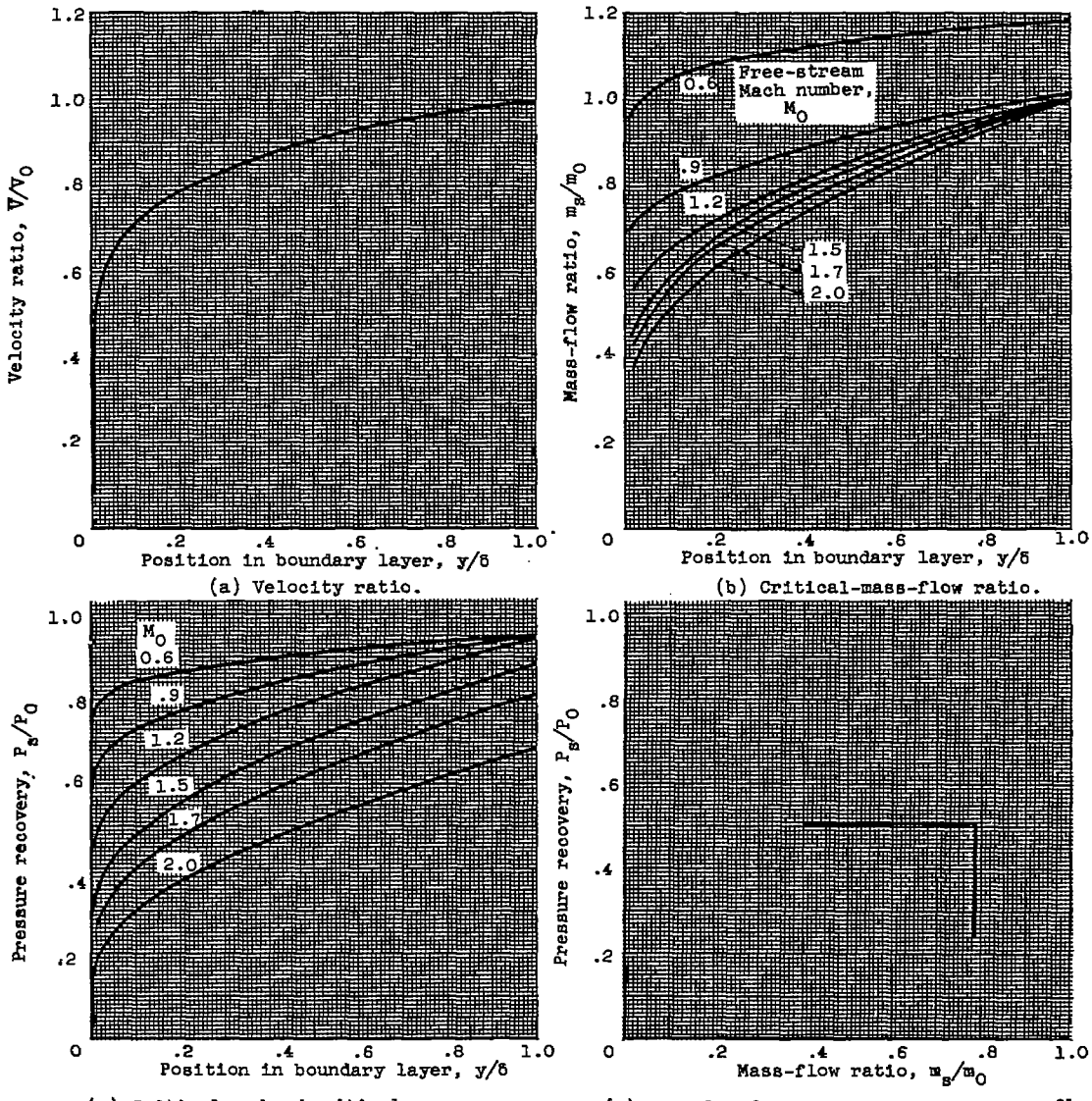

(a) Velocity ratio.

(b) Critical-mass-flow ratio.

(c) Critical and subcritical pressure recovery.

(d) Example of pressure-recovery - mass-flow characteristics. Free-stream Mach number, 2.0; distance ratio, 0.5.

Figure 10. - Computed inlet performance.

[redacted]

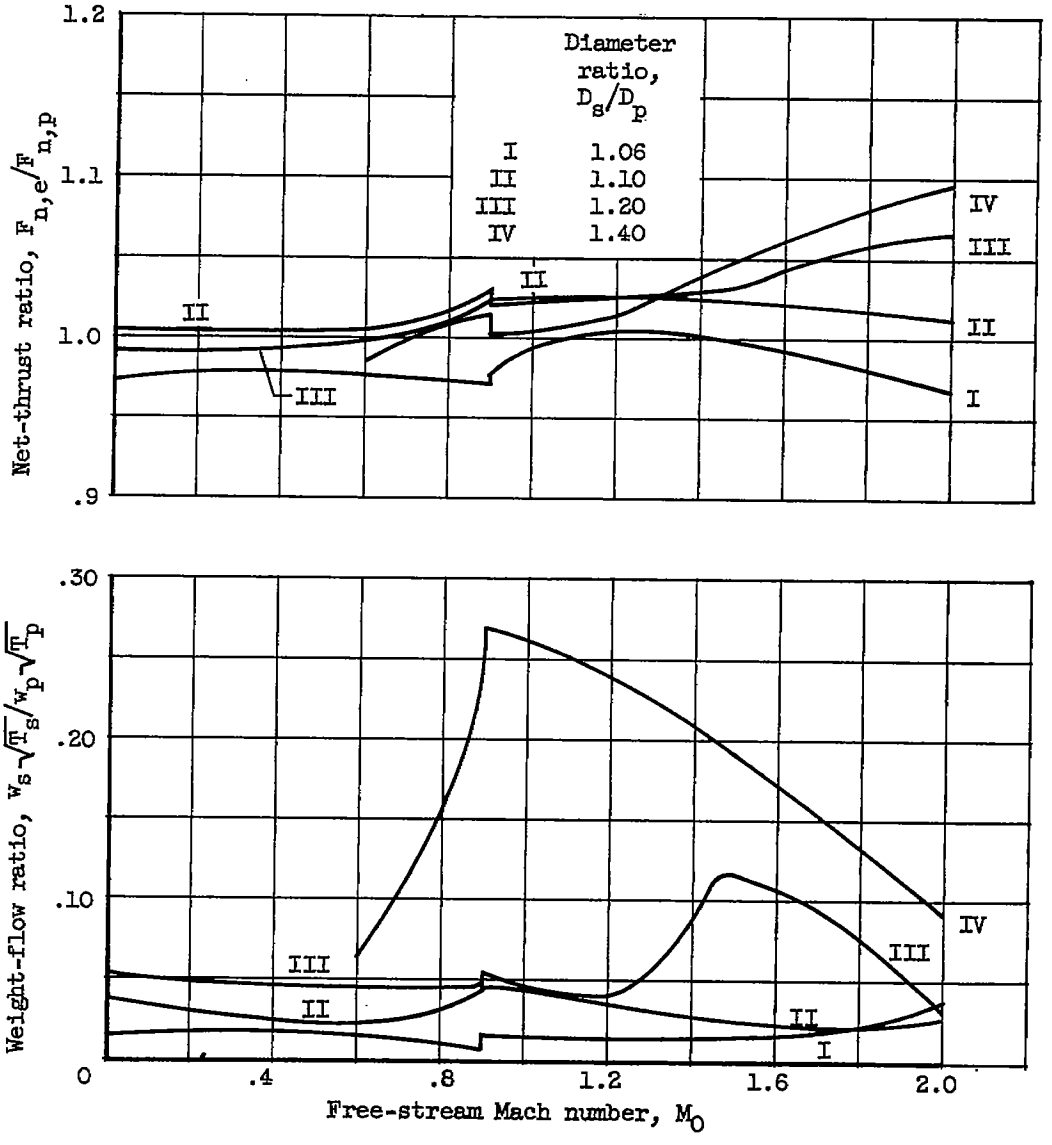

Figure 11. - Series of fixed-diameter-ratio ejectors matched to variable inlets. Spacing ratio, 0.80.

3666

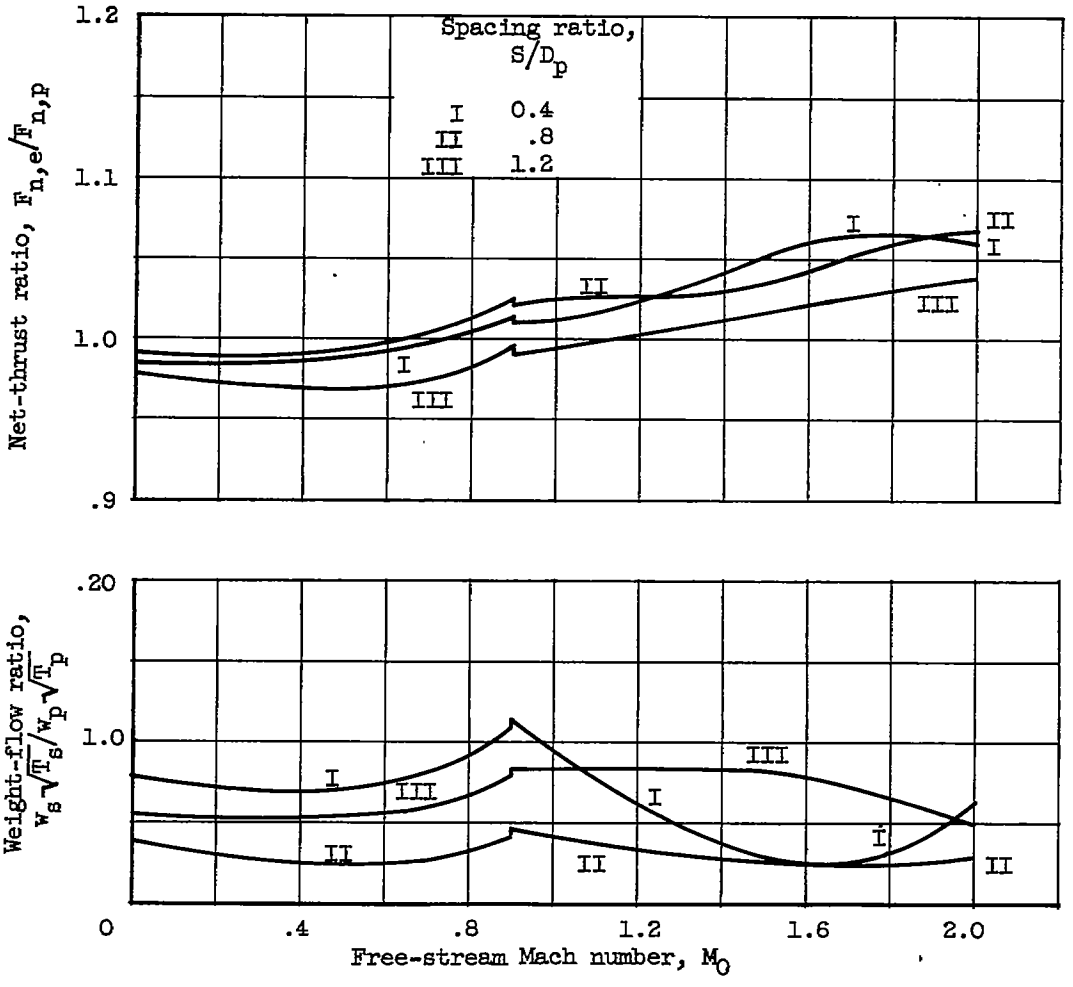

Figure 12. - Series of fixed-spacing-ratio ejectors matched to variable inlets. Diameter ratio, 1.20.

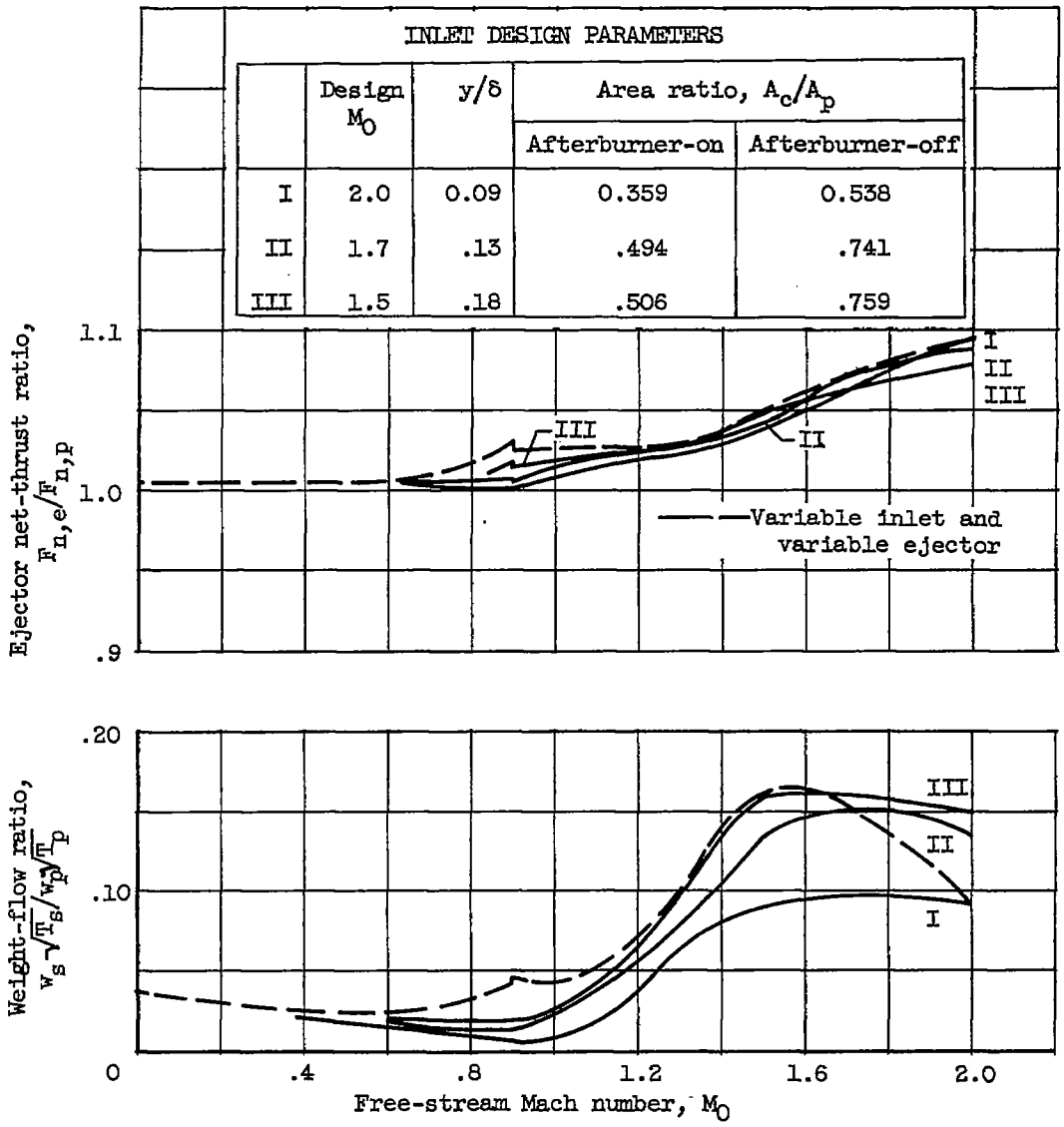

Figure 13. - Penalty encountered with fixed-inlet and variable-diameter-ratio ejector designed for peak performance. Spacing ratio, 0.80.

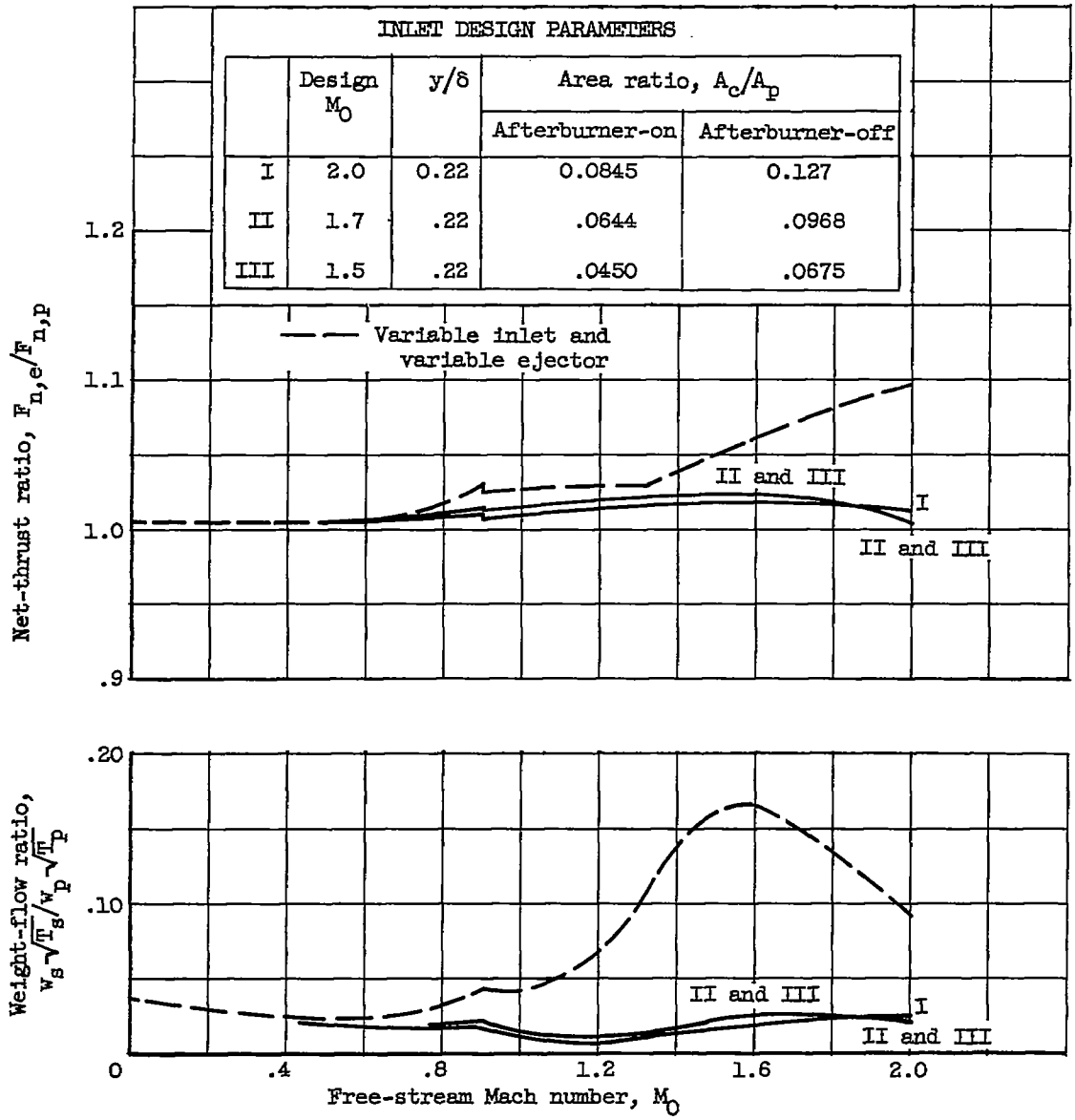

(a) Diameter ratio, D_s/D_p, 1.10.

Figure 14. - Comparison of fixed inlets and fixed ejectors with variable inlets and variable-diameter-ratio ejectors. Spacing ratio, 0.80.

[redacted]

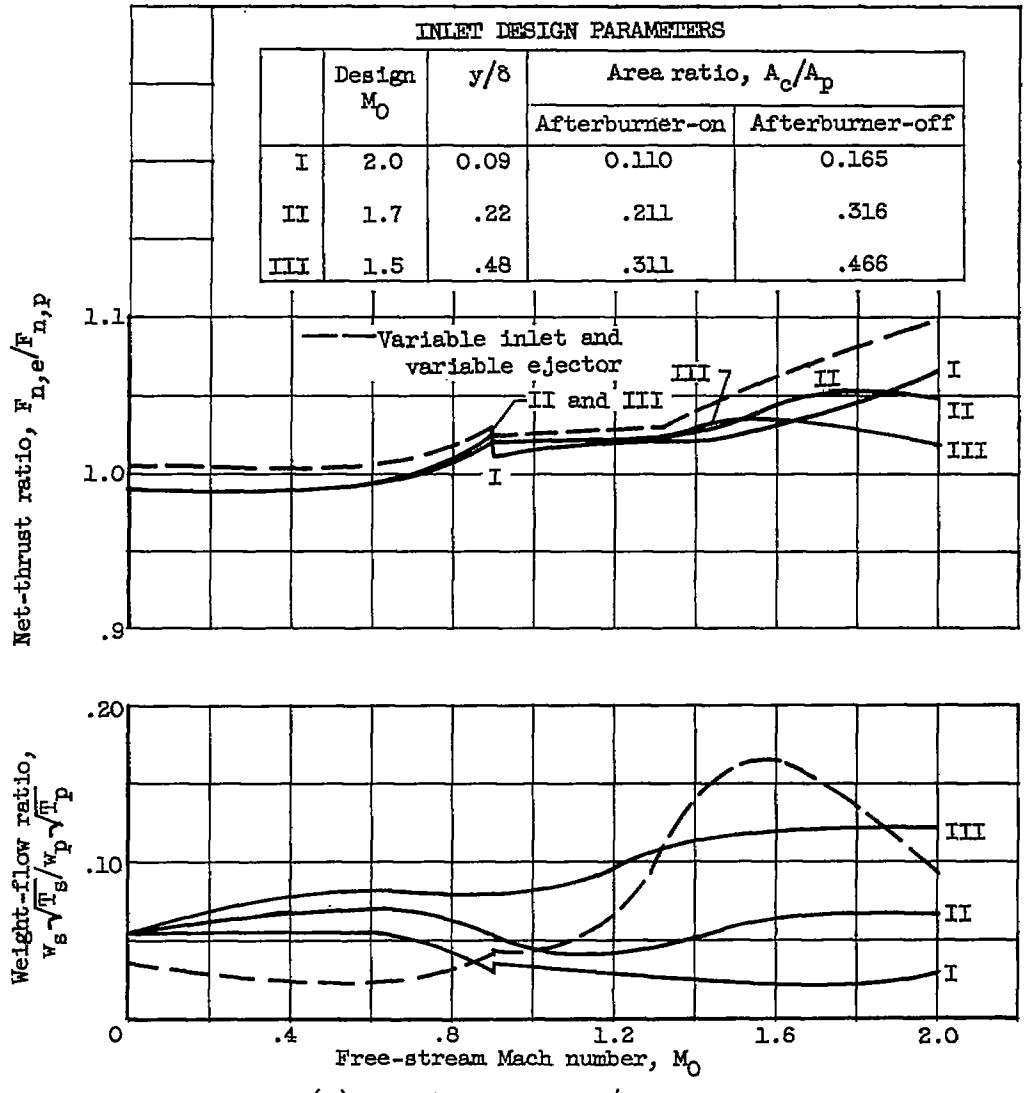

(b) Diameter ratio, D_s/D_p, 1.20.

Figure 14. - Continued. Comparison of fixed inlets and fixed ejectors with variable inlets and variable-diameter-ratio ejectors. Spacing ratio, 0.80.

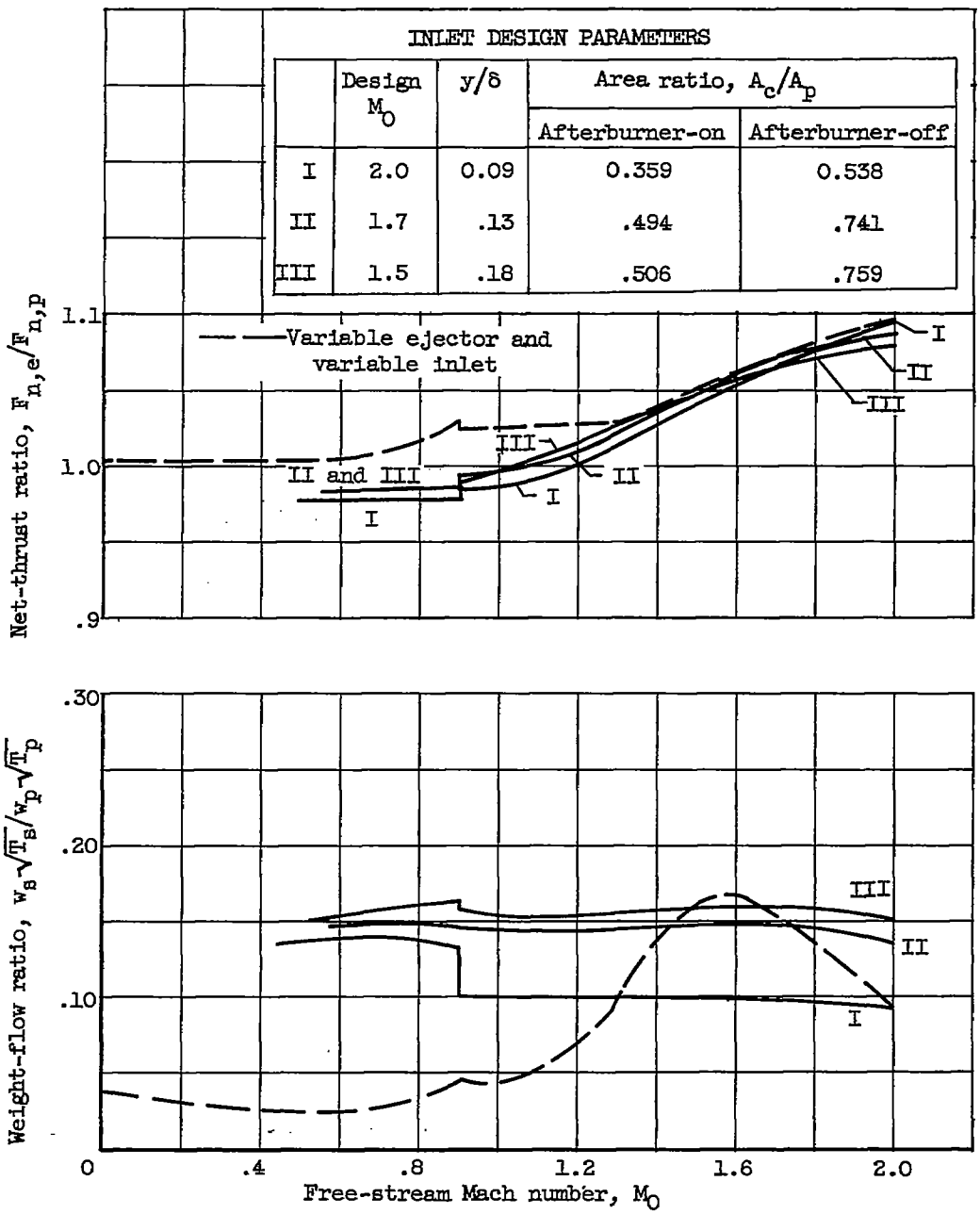

(c) Diameter ratio, D_s/D_p, 1.40.

Figure 14. - Concluded. Comparison of fixed inlets and fixed ejectors with variable inlets and variable-diameter-ratio ejectors. Spacing ratio, 0.80.

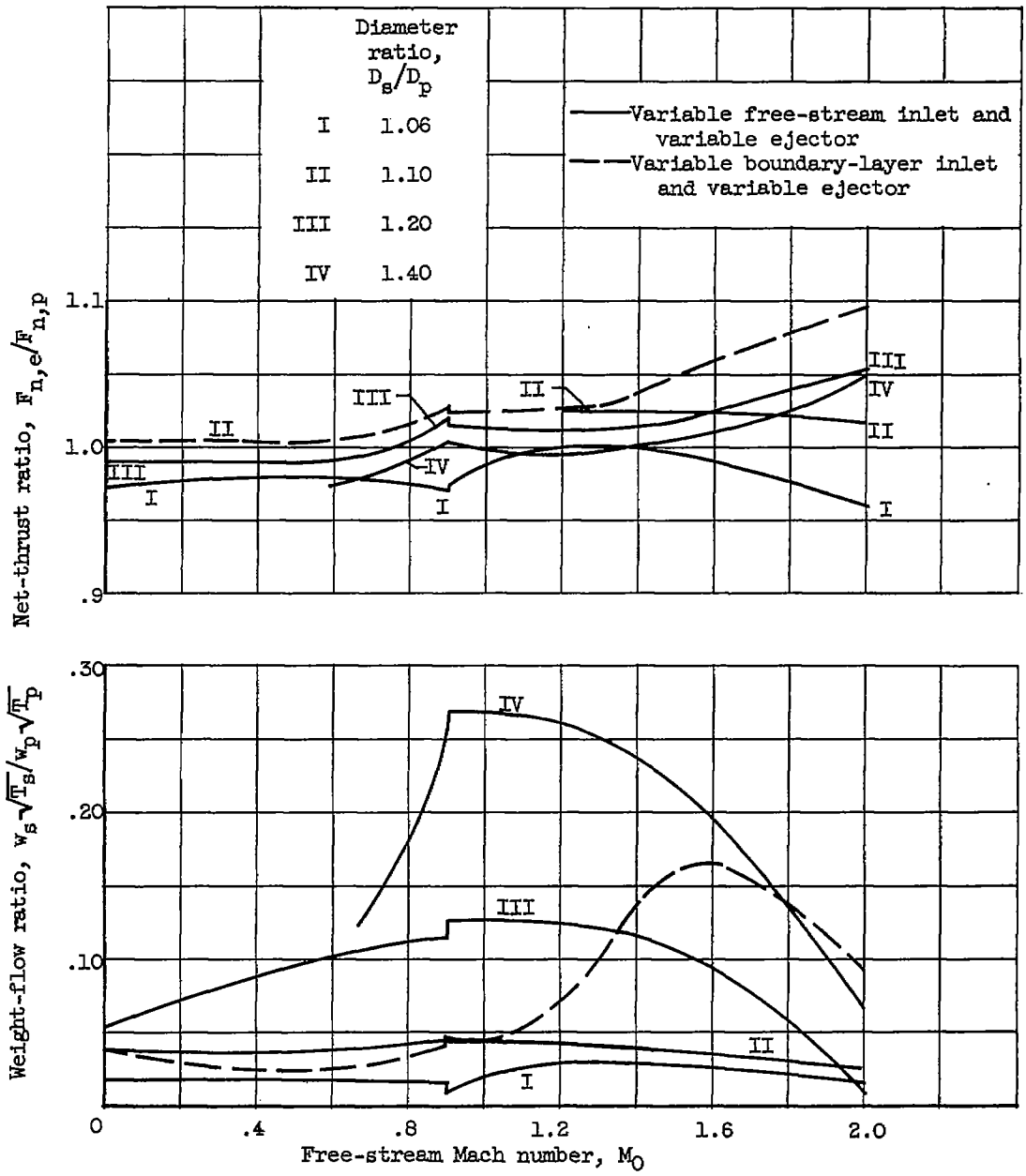

Figure 15. - Maximum performance obtainable with variable-diameter-ratio ejector and variable-size free-stream inlet. Spacing ratio, 0.80.

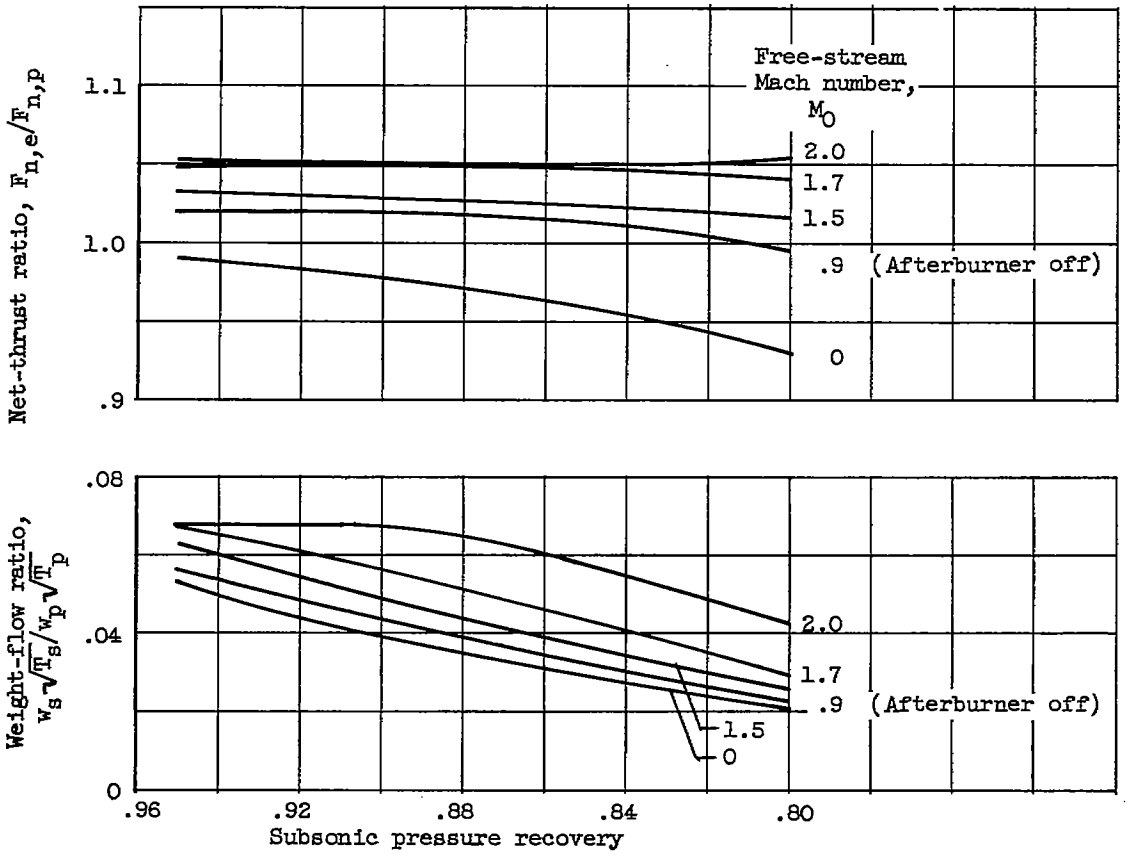

Figure 16. - Effect of subsonic total-pressure losses on performance with fixed configuration. Design free-stream Mach number, 1.7. Diameter ratio, 1.20; spacing ratio, 0.80.

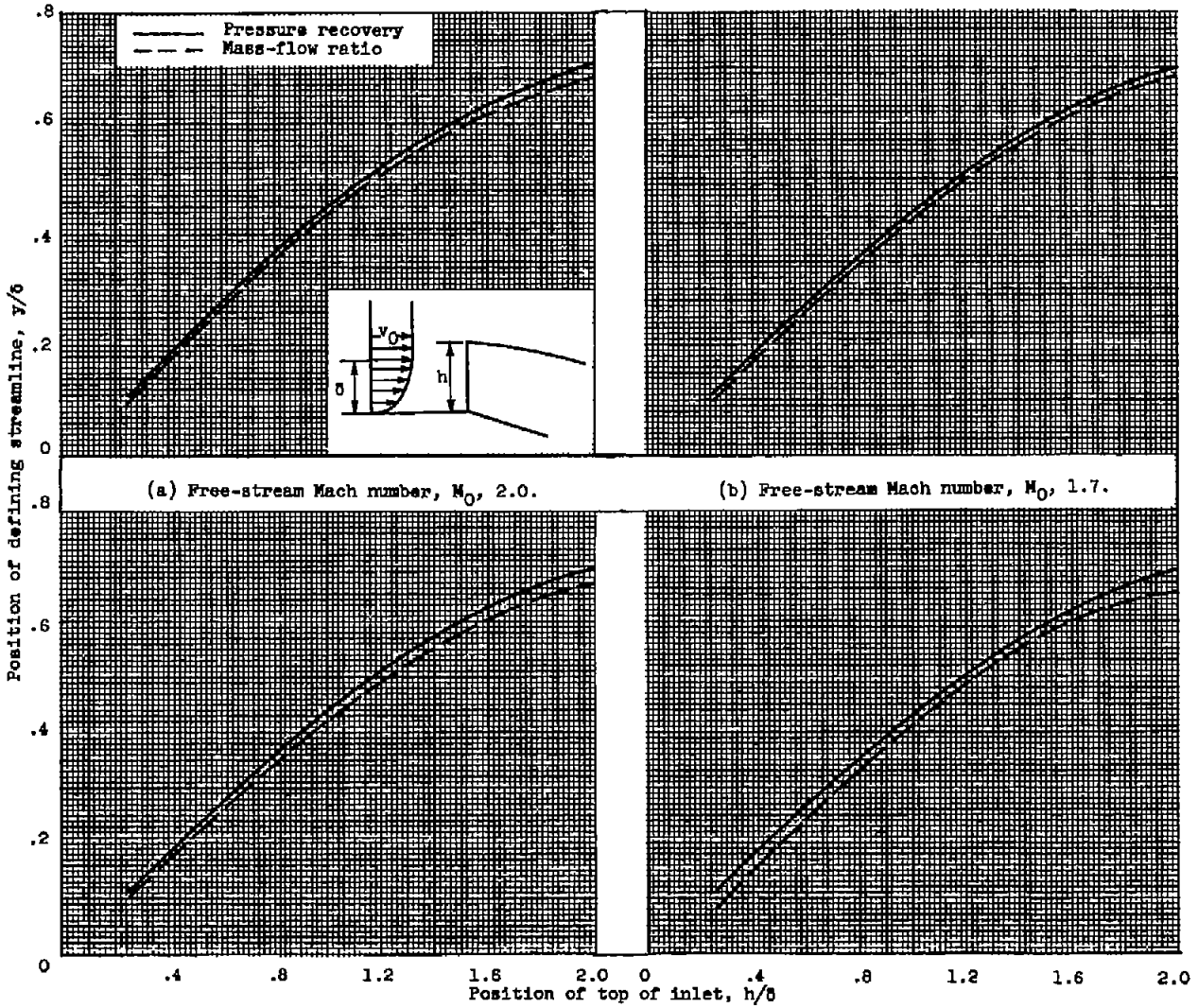

Figure 17. - Comparison of filament position and attached inlet height for equivilent performance.

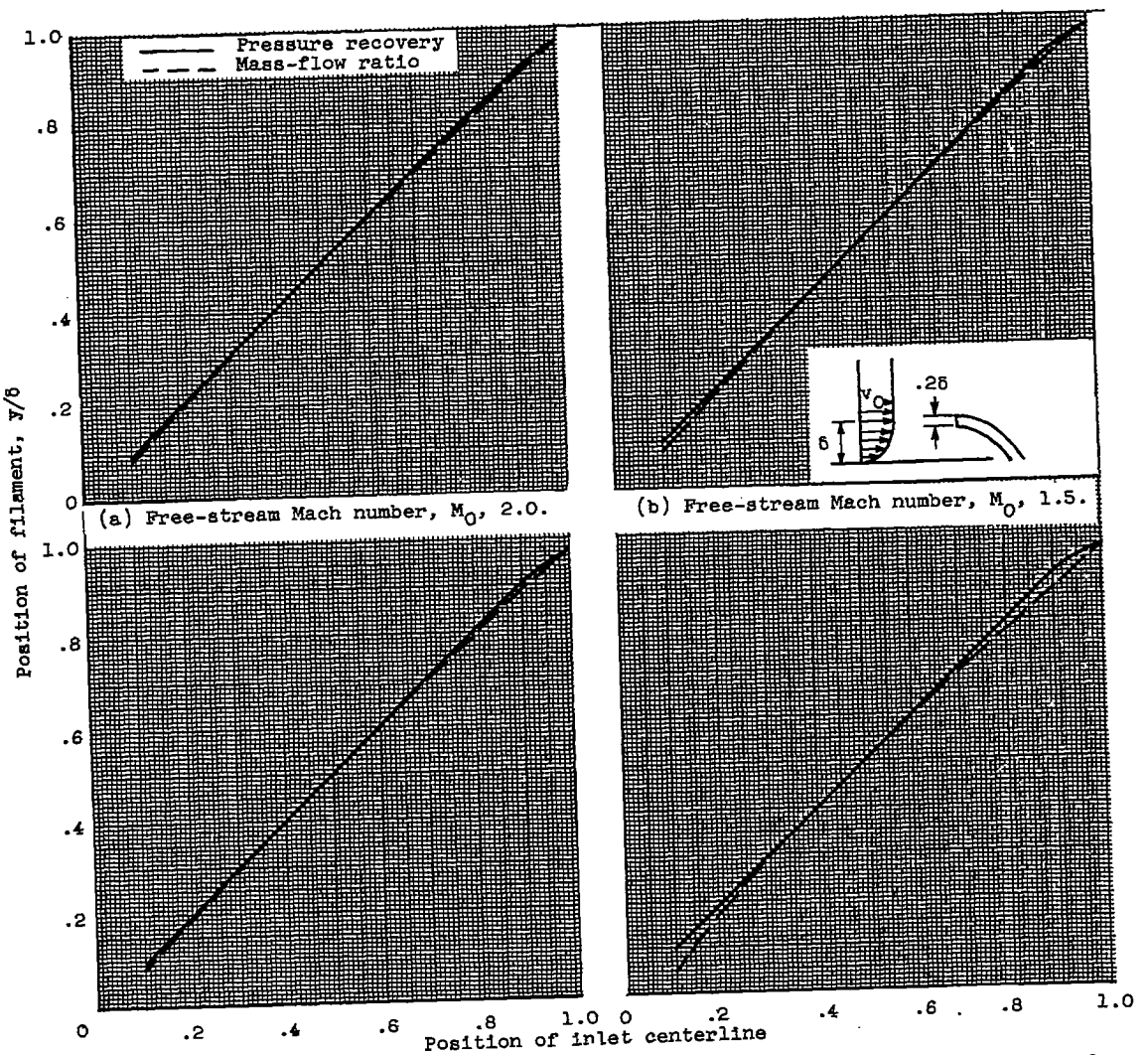

Figure 18. - Comparison of filament position and unattached inlet centerline for equivalent performance. Inlet height, 0.25.